Journal of Marine Research, 68, 881–920, 2010

When and why does bioturbation lead to diffusive mixing?

by Filip J. R. Meysman[1,2,3], Bernard P. Boudreau[4] and Jack J. Middelburg[2,5]

ABSTRACT

Bioturbation in aquatic sediments results from many different biological activities, inducing particle displacement over a variety of length and time scales. Despite this inherent complexity, empirical tracer studies show that bioturbational mixing is often well described by a simple diffusive model. To resolve this apparent contradiction between biological complexity and modeling simplicity, we present an investigation into the diffusive nature of bioturbation. To this end, we examine a stochastic description of bioturbation, where particle mixing is described as a sequence of random bioturbation events. Particle movement is governed by three basic variables: the direction of jumping, the jumping distance, and the waiting time between two bioturbation events. A set of gradually more complex random-walk models is constructed by treating these variables consecutively as stochastic. Each time, the conditions are determined under which these random walks generate diffusive behavior. One important criterion is that the tracer should experience a sufficient number of bioturbation events, and so the time scale of observation should be large enough. The full list of conditions needed to arrive at diffusive mixing is different and more extensive than in past examinations of the topic. This analysis clarifies the relation between the biodiffusion model and more sophisticated mixing models, revealing that the conventional distinction between local and nonlocal models is not entirely relevant. Instead, we propose a distinction between "normal" or "anomalous" mixing, which is based on the intrinsic nature of the faunal activities causing particle dispersal. Overall, our analysis provides insight into the conditions under which the biodiffusion model can be applied to tracer profiles, and also shows why it sometimes fails, as is the case of sediments dominated by head-down deposit feeders.

1. Introduction

The term bioturbation refers to the biological reworking of sediments (Richter, 1952), and more specifically, to the displacement of solid particles caused by a variety of biological activities, such as locomotion, feeding, and burrows construction (Meysman *et al.,* 2006). Bioturbation forms the dominant transport mode for reactive compounds in the sediment environment, affecting the distribution of organic matter, iron- and manganese

1. Department of Analytical and Environmental Chemistry, Earth System Sciences Research Unit, Vrije Universiteit Brussel, Pleinlaan 2, 1050 Brussel, Belgium.
2. The Netherlands Institute of Ecology (NIOO-KNAW), Centre for Estuarine and Marine Ecology, Korringaweg 7, 440l NT Yerseke, The Netherlands.
3. Corresponding author. ***email: f.meysman@nioo.knaw.nl***
4. Department of Oceanography, Dalhousie University, Halifax, NS B3H 4J1, Canada.
5. Department of Geochemistry, Faculty of Geosciences, University of Utrecht, The Netherlands.

hydroxides, and other solid-bound compounds, such as radionuclides and contaminants (Aller, 1982). Therefore, it should be included as a standard transport process in reactive transport models of aquatic sediments (Berner, 1980; Boudreau, 1997); hence, one needs an adequate process model of particle transport induced by bioturbation (Matisoff, 1982; Aller, 1988; Boudreau, 2005).

At present, the standard description of bioturbation is based on the biodiffusion analogy, originally introduced by Goldberg and Koide (1962), and popularized by Guinasso and Schink (1975). The biodiffusion analogy essentially states that Fick's laws of diffusion are applicable to bioturbation (Boudreau, 1986). The biodiffusion model is attractive due to its inherent simplicity. It reduces the complex phenomenon of biological mixing to a single convenient parameter, the biodiffusion coefficient D_b. Furthermore, the governing tracer conservation equation becomes the well-known diffusion equation, for which analytical solutions are readily available (Crank, 1975; Boudreau, 1997). This way, values for D_b can be estimated straightforwardly by fitting regression lines to down-core profiles of specific tracers. As a result, the biodiffusion model has been employed overwhelmingly in the sediment literature. Currently, it forms the default formulation in radiotracer studies (e.g. Cochran, 1985; Soetaert *et al.,* 1996; Mulsow *et al.,* 1998; Crusius and Kenna, 2007), pulse-tracer experiments (e.g., Solan *et al.,* 2004; Fernandes *et al.,* 2006; Maire *et al.,* 2007) and general diagenetic models (e.g. Boudreau, 1989; Van Cappellen and Wang, 1996; Berg *et al.,* 2001; Meysman *et al.,* 2005).

Nevertheless, the status of the biodiffusion model remains partly controversial (Reed *et al.,* 2006, 2007; Lecroart *et al.,* 2010). In the eyes of its critics, the biodiffusion analogy is plainly too simple in its assumptions. The biodiffusion model is traditionally justified by assuming that particles experience a random walk with a fixed step length and fixed step frequency. In the limiting situation where particle movement becomes local, i.e., when the step length becomes very small and the step frequency very high, one then retrieves the biodiffusion equation (Wheatcroft *et al.,* 1990; Meysman *et al.,* 2003; see also below). Yet, the stringent requirements for (infinitely) frequent and small displacements have made biologists uncomfortable. Indeed, given the existing knowledge about life-history and ecology of bioturbating organisms, one would expect a wide range of spatio-temporal scales on which particles are displaced, not only small and frequent ones. Consequently, the biodiffusion model has been criticized for its lack of biological realism (e.g. Francois *et al.,* 1997). In response, more complex bioturbation models have been advanced, which claim to possess sounder biological foundations. These so-called nonlocal models allow long-range mass transfer between spatially separated layers within the sediment, and are usually advocated as a more realistic description of bioturbation (Boudreau and Imboden, 1987; Francois *et al.,* 2001). However, these nonlocal descriptions typically lead to integro-differential equations, which require non-standard numerical solution methods (Boudreau and Imboden, 1987; Meysman *et al.,* 2003). As a result, nonlocal models are noticeably less popular and have only been implemented sporadically (e.g. Rice, 1986; Shull, 2001; Solan *et al.,* 2004; Delmotte *et al.,* 2007).

Despite its apparent lack of biological realism, the biodiffusion model remains the model of choice in most practical applications. Besides its mathematical simplicity, another important reason for its popularity is that the biodiffusion model has proven to be an accurate *empirical* model. Indeed, a fair proportion of radio-tracer field data in bioturbated sediments can be well fitted by steady-state solutions of the biodiffusion model. This is especially true for long-lived tracers like the frequently used ^{210}Pb (with a half life of 22.4 years). For short-lived radio-tracers and short-term pulse tracer experiments with conservative tracers, the match between biodiffusion model and data is not always obvious (Reed *et al.,* 2007; Meysman *et al.,* 2008b). Nonetheless, in many circumstances, the data seem to prove that the biodiffusion model does work. This remarkable situation has been previously referred to as the "biodiffusion paradox" (Meysman *et al.,* 2003): why does the biodiffusion model work for bioturbation, when the underlying assumption of small-scale transport seems to be violated?

The biodiffusion model remains an important tool in sediment geochemistry, and so, the prime aim of this communication is to clarify the uncertainty regarding its validity and applicability. Building upon the results of recent theoretical investigations of bioturbation (Reed *et al.,* 2006, 2007; Meysman *et al.,* 2008a,b), we show here that the "biodiffusion paradox" results from a misinterpretation of the conditions under which bioturbation can be treated as a diffusive process. We will show that the dichotomy between the "local" biodiffusion model and more sophisticated "nonlocal" models is artificial. This is done by means of an in depth mathematical analysis of particle dispersal, in which we address the following questions. [1] What are the exact assumptions underlying the biodiffusion model? [2] How does one account for biological variability in bioturbation models? [3] Can we provide an explicit link between biological activity and the biodiffusion coefficient? [4] What is the relation between the biodiffusion model and more complex models? [5] How to explain the "diffusive" character of down-core tracer profiles? [6] When can one apply the biodiffusion model, and when is it necessary to apply more sophisticated models? To answer these questions, we will employ a recently developed stochastic description of bioturbation (Meysman *et al.,* 2008a) and construct a set of gradually more complex random-walk models. In each case, we will investigate the conditions under which the random-walk model reduces to the biodiffusion model. In doing so, we will point out some weak points and inconsistencies in past model treatments of bioturbation. In a final part, our mathematical results are interpreted and translated in terms of their implications for practical tracer studies.

2. Stochastic description of bioturbation

From the perspective of a particle, displacement due to bioturbation can be regarded as resulting from a sequence of bioturbation events (e.g. the infilling of a burrow, the passage of a burrowing organism). Within a bioturbation event, a particle "jumps" to a new location, and subsequently it "waits" at this location until the next bioturbation event occurs. Formally, a bioturbation event is thus constrained by three variables: (1) the

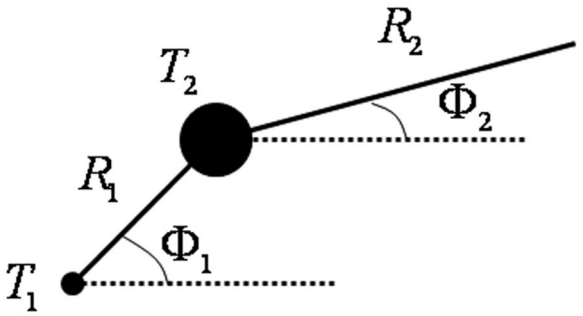

Figure 1. Schematic diagram of two consecutive bioturbation events. T = waiting time (as indicated by radius of starting point). R = jump length. Φ = jump angle.

waiting time T between two consecutive bioturbation event (2) the direction of travel, which can be formalized by the jump angle Φ with respect to some fixed coordinate system (the number of jump angles depends on the dimensionality of the problem), and (3) the jump distance R, which a particle travels in a given direction during a bioturbation event (Fig. 1).

Because many different organisms inhabit the sediment, and each organism displays a variety of locomotion, feeding and burrowing activities, the jump distance, jump direction and waiting time will vary between bioturbation events. During one such event a particle may travel over small or large distances. Similarly, the next bioturbation event may follow quickly, but equally, the particle could remain undisturbed for a rather long time interval. To account for such variability, one can adopt a stochastic perspective, assuming that the interplay between particles and biological activity is sufficiently erratic, so that bioturbation events may be considered as random processes. This stochastic model approach to bioturbation was discussed in detail in Meysman *et al.* (2008a), and only the main points are repeated here. The bottom line is that the jump distance R, the jump angle Φ and the waiting time T are all modeled as stochastic variables, each represented by a probability distribution function (PDF). The so-called *waiting-time distribution*

$$\Psi_T(\tau)d\tau = \Pr\{\tau < T < \tau + d\tau\} \tag{1}$$

then defines the probability (indicated as Pr{. . .}) that a bioturbation event will occur in the time interval $(\tau, \tau + d\tau)$. Similarly, the jump-angle distribution

$$\Psi_\Phi(\phi)d\phi = \Pr\{\phi < \Phi < \phi + d\phi\} \tag{2}$$

describes the probability that a particle will be displaced in a certain direction $(\phi, \phi + d\phi)$. The walk is termed "directionally random" when all jump angles are equally probable (i.e., a uniform jump-angle distribution). Finally, the jump-distance distribution

$$\Psi_R(\rho)d\rho = \Pr\{\rho < R < \rho + d\rho\} \tag{3}$$

defines the probability a particle will travel a distance within the range $(\rho, \rho + d\rho)$ during a given event. The walk is termed "isotropic" when the jump-distance distribution is the same for all directions. Together, the three probability distribution functions given by (1)–(3) provide a stochastic model for displacement of a particle within a single bioturbation event. In the next sections, we will analyze different random walk models that are all based on this stochastic jumping-and-waiting formalism. Each time we will investigate if, when and how these random walk models reduce to the classical diffusion equation.

Our main goal is to show a proof-of-concept, and therefore, it is desirable to keep the complexity of the mathematical expressions at bay. In order to reduce the problem to its barest essentials, we adopt some suitable idealizations. Firstly, we only consider particle transport in the vertical direction, and so, particles are moved along the x-coordinate axis, where x represents depth into the sediment. The extension to multiple dimensions is rather straightforward and is not essential for the present discussion. In a one-dimensional setting, the jump angle Φ can only take two values: down ($\Phi = 0$) and up ($\Phi = \pi$). The associated jump-angle distribution becomes

$$\Psi_{\Phi}(\phi) = p\delta(\phi) + (1 - p)\delta(\phi - \pi) \tag{4}$$

where p denotes the probability that a particle moves downward, and $\delta(\ldots)$ is the Dirac delta function. When $p = 1/2$ the particle has equal chances of moving up or down, and the random walk is directionally random. In a one-dimensional random walk, the jump angle Φ and jump distance R are often combined into the jump length L, which describes both the direction and distance a particle travels. Note that this jump length may not be interpreted as a *distance,* as its value can either be positive or negative. The value of L is positive when the direction of the jump coincides with the direction of the x-axis (particles move downward into the sediment), and negative otherwise (particles moving upwards). The associated *jump-length distribution* is then given by

$$\Psi_L(\lambda)d\lambda = \Pr\{\lambda < L < \lambda + d\lambda\}. \tag{5}$$

When the random walk is both isotropic and directionally random, the jump-length distribution becomes symmetric, i.e. $\Psi_L(\lambda) = \Psi_L(-\lambda)$. In the derivations below, we will assume that particle displacement is isotropic, but not necessarily directional random, and so p can be different from 1/2 in (4). As we will discuss below, the constraints of isotropy and directional randomness are not essential for the biodiffusion model.

3. Constraints on the bioturbation fingerprint

The displacement of a particle within a single bioturbation event is now governed by two probability distributions functions, i.e. the waiting-time distribution from (1) and the jump-length distribution from (5). Together, these are referred to as the "bioturbation fingerprint" of the bioturbation activity at a given location (Meysman *et al.,* 2008a). Note that this separation between waiting-time and jump-length distribution already entails

some important underlying assumptions. It is worthwhile to start out a bit more general, and consider these constraints explicitly, since they are critical in obtaining diffusive behavior. In the most general case, the bioturbation fingerprint can be represented by a joint probability distribution, which describes how a given bioturbation event works. Technically, this joint probability distribution specifies the probability that a particle waits for a period τ and then takes a step of length λ when it is located at depth x in the sediment at the current time t

$$\Psi(\lambda, \tau; x, t, t' < t) \equiv \Pr\{\lambda < L < \lambda + d\lambda, \tau < T < \tau + d\tau; x, t, t' < t\}. \tag{6}$$

In the derivations below, we will use three simplifying assumptions that are needed to arrive at diffusive behavior.

1. *Successive bioturbation events must be independent (Markov assumption).*
2. *Successive bioturbation events are characterized by the same bioturbation fingerprint (Translational invariance of waiting time and step length distribution).*
3. *Statistical independence of jumping behavior from the waiting behavior, i.e., jump distances and waiting times are not correlated.*

The Markov assumption implies that the way in which particles are displaced within a given bioturbation event does not depend on the past history of the mixing at the site. Each bioturbation event must act as an independent random event, and so the overall mixing process lacks "memory." Mathematically this implies that the bioturbation fingerprint can only be dependent on the current time t and not on any previous times $t' < t$

$$\Psi(\lambda, \tau; x, t, t' < t) = \Psi(\lambda, \tau; x, t). \tag{7}$$

When considering faunal mixing in sediments, there is little indication that past events will substantially influence how a particle is displaced in the current mixing event. Non-markovion dispersal is usually associated with self-avoidance, where particles refuse to visit a site where they have been before. One could imagine that deposit feeders will avoid the ingestion (and hence transport) of particles that have already been ingested before, but overall, we believe that such avoidance mechanisms are relatively weak. So in terms of bioturbation, the Markov assumption does not seem too problematic.

Compared to the above conditions, the requirement that successive mixing events should be characterized by the same bioturbation fingerprint is a far more drastic assumption. In the random walk literature, this condition usually demands that random walks should have identically distributed steps (Hughes, 1995). This so-called translational invariance of mixing implies that the joint probability distribution is no longer dependent on the time t and the depth x

$$\Psi(\lambda, \tau; x, t) = \Psi(\lambda, \tau). \tag{8}$$

In reality, the density and activity of fauna typically varies with depth and shows lateral patchiness and is marked by seasonal and decadal variability (Herman *et al.,* 1999; Lecroart *et al.,* 2007). Such trends cannot be disregarded and must be considered a characteristic feature of faunal mixing under natural conditions. However, these trends are not really problematic as long as temporal and spatial changes are sufficiently smooth. In other words, the actual mode of mixing should not exhibit abrupt changes with depth and time. For some mixing types (e.g. moving and ploughing through the sediment), this condition seems valid. Yet, for other important mixing activities, like head-down deposit feeding, there will be abrupt changes in the step length distribution with depth (see below). In the discussion section, we will come back to this important assumption, and examine the consequences when the assumption of translational invariance no longer holds.

The third constraint requires a jumping behavior that is statistically independent from the waiting behavior. As noted in Meysman *et al.* (2008a), this condition does not seem problematic for most bioturbation activities. There is no immediate reason to suspect a correlation between the distance over which a particle is displaced and the time this particle waits between two bioturbation events. Statistically, it implies that the joint probability distribution can be expressed as the product of a separate waiting time and step length distribution

$$\Psi(\lambda, \tau) = \Psi_L(\lambda)\Psi_T(\tau). \tag{9}$$

To describe the reworking in a natural sediment context, the above assumptions may be too restrictive. Meysman *et al.* (2008a) already provide a detailed discussion of the justifiability of some these constraints, and we will return to this important issue in the discussion section. Note, however, that the prime goal here is to investigate the conditions under which particle mixing becomes diffusive. In the derivations below, the above three simplifying assumptions will be required to arrive at such diffusive behavior. Accordingly, when these assumptions break down, random walks can exhibit a different, nondiffusive behavior.

4. Discrete-time discrete-space (DTDS) description

The trajectory of a sediment particle ultimately results from the consecutive bioturbation events. In each such bioturbation event, the particle receives a new value for the jump distance R, the jump angle Φ and the waiting time T. The result is that the particle will perform a random walk. Random walk theory contains various types of random walks, and it is important to understand these in order to predict where a particle eventually will end up (Fig. 2). If all the values T, Φ, and R are fixed (or equally T and L), there is no randomness. Particles will always move in straight line, and the resulting walk is termed *ballistic* (Fig. 2a). To arrive at a true random walk model, one or more variables need to be stochastic. Depending on the actual number of parameters that are considered stochastic, different random walk models can be developed.

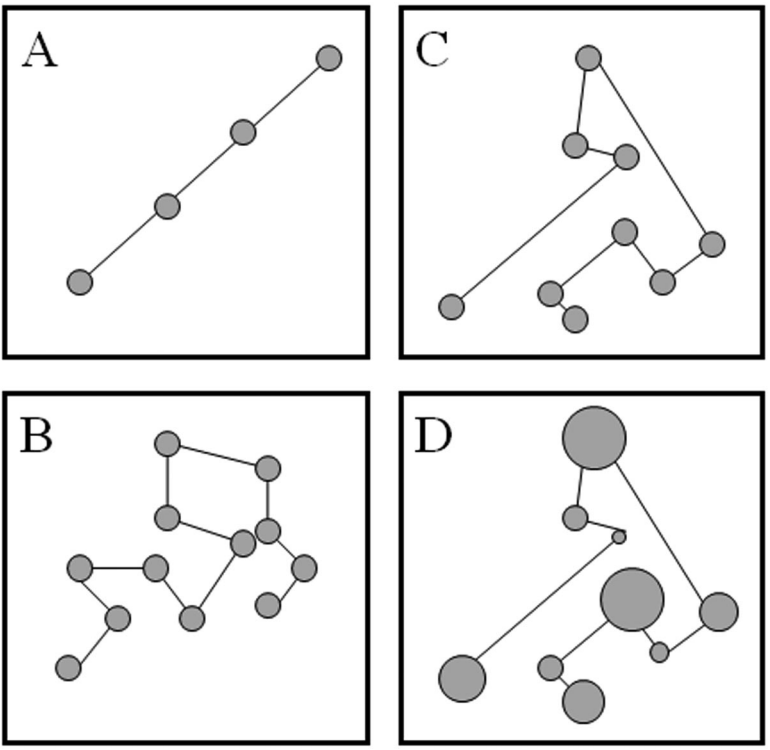

Figure 2. Four different random walks. (A) Ballistic (B) Pearson (discrete time discrete space) (C) Bachelier (discrete time continuous space) (D) Montroll-Weiss (continuous time continuous space). The radius of the circles denotes the length of the waiting time.

Presumably the most familiar random walk is where the walker always takes steps of the same length at constant time intervals (Fig. 2b). In other words, the random walker is disoriented and chooses a random direction at each new step, but does not lose control over his stepping frequency and stride length, which are both fixed. We refer to this process as a *discrete-time discrete-space (DTDS) random walk,* since the waiting time T and the jump distance R are fixed, deterministic quantities. The only random aspect remaining is the direction of travel: the jump angle Φ constitutes a stochastic variable governed by the jump angle distribution in (2). In the case of directional randomness, a particle has an equal probability of going in all directions (the jump angle Φ is uniformly distributed). The original "random walk" model coined by Pearson (1905) described the invasion of cleared jungle regions by mosquitoes and constituted an isotropic, directionally random DTDS process in two dimensions—see Hughes (1995) for an entertaining historical discussion.

a. Bioturbation as a Pearson walk

The first applications of random walks to bioturbation were also based on the isotropic, directionally random DTDS process (Boudreau, 1989; Wheatcroft *et al.,* 1990; Swift *et al.,* 1996). These authors proposed that particle dispersal could be modeled on a regular lattice of spacing λ_c, where sediment particles move to adjacent sites at equal time intervals τ_c. This lattice DTDS process can be parsed into the general stochastic formalism of (1) and (5) when adopting "pulsed" waiting time and "pulsed" jump-length distributions

$$\Psi_T(\tau) = \delta(\tau - \tau_c) \tag{10}$$

$$\Psi_L(\lambda) = (1/2)\delta(\lambda - \lambda_c) + (1/2)\delta(\lambda + \lambda_c) \tag{11}$$

where $\delta(u)$ represents the Dirac delta function. This DTDS process assumes that bioturbation events are independent, always characterized by the same distributions (10) and (11), and that waiting and jumping behavior is independent. Within a given bioturbation event, particles are moved with a fixed jump length λ_c and a fixed waiting time τ_c between displacements. The only random aspect remaining is the direction of travel. The factor 1/2 in the jump length PDF (11) indicates that particles have equal chances of moving upwards or downward in the sediment (directional randomness). For a particle originally released at the origin, we can now track its position after consecutive bioturbation events. The probability $P_{N,j}$ of finding this particle at lattice site j after N bioturbation events is given by the simple recursion relation

$$P_{N+1,j} = \frac{1}{2}\left[P_{N,j-1} + P_{N,j+1}\right]. \tag{12}$$

The one-dimensional, isotropic Pearson walk given by (12) provides the most simple random walk mechanism of bioturbation. It also forms the classical starting point for the derivation of the diffusion equation. Such "continuum limit" derivations have been presented for biological applications in general (Berg, 1993; Murray, 1989; Okubo and Levin, 2001), as well as for the specific case of bioturbation (Wheatcroft *et al.,* 1990; Meysman *et al.,* 2003). Here we revisit this "continuum limit" derivation, but our approach will differ at two key points from past treatments. Firstly, in past treatments, the continuum limit is typically presented as a single step operation. Here, we emphasize that continuum limit is reached via three separate steps, i.e., the application of [1] the Law of Large numbers, [2] the continuum approximation, and [3] the long-time limit. Secondly, our justification of the third step (the long-time limit) will be different from past treatments. In the next sections, we sketch an outline of the reasoning, while the mathematical details are presented in Appendix C.

b. The Law of Large Numbers

The simple Pearson walk of (12) provides a description of bioturbation at the microscopic level: it is a *stochastic model* for evolution of the *position* of a *single particle.* Yet, in order to analyze tracer data gathered in field and laboratory experiments, one needs a description at the macroscopic level. In other words, one requires a *deterministic model* for the evolution of the *concentration profile* of an ensemble of many particles. To go from the "stochastic/single particle" level to the "deterministic/many particles" level, one needs to invoke the Law of Large Numbers (Feller, 1968). This allows the $P_{N,j}$ to be swapped for the concentration $C_{N,j}$, so that the recursion relation (12) becomes

$$C_{N+1,j} = \frac{1}{2}\left[C_{N,j-1} + C_{N,j+1}\right]. \tag{13}$$

For a process that has a probability p of success in each trial, the Law of Large Numbers states that in a series of repeated trials, the percentage of successes will converge towards p as the number of trials becomes large. In our case, the repeated trials are due to the many particles that make up the concentration profile. If particles are moving independently, the Law of Large Numbers predicts that the concentration profile will attain the same form as the probability distribution describing a single particle's position. Note that the assumption of independent movement of particles is a strong assumption. In actual bioturbation activities, fauna will move whole packages of sediment, thus displacing all particles within one such package collectively (and hence, not independently). Only as the number of bioturbation events increases, particles will gradually start to move independently from each other.

c. The continuum approximation

Eq. (13) is still a "discrete" equation in the sense that the concentration is only defined at discrete points in time and space. For applications, it is useful to derive a continuum counterpart, which exists at each point in time and space. The first step in the transition from the discrete to the continuum level is to replace the discrete concentration $C_{N,j}$ with an equivalent continuous-space and continuous-time approximation $C(x, t)$, so that the equality $C(x, t) = C_{N,j}$ holds at every lattice point $x = j\lambda_c$ and at every time step $t = N\tau_c$. This way, (13) transforms to

$$C(x, t + \tau_c) = \frac{1}{2}\left[C(x - \lambda_c, t) + C(x + \lambda_c, t)\right]. \tag{14}$$

Being continuous quantities, one can now expand the concentrations on both sides of (14) in a Taylor series. After some rearrangement (see Appendix A), (14) can be recast into the "pseudo-diffusive" form

$$\frac{\partial C}{\partial t} = \left\{\frac{1}{2}\frac{\lambda_c^2}{\tau_c}\right\}\frac{\partial^2 C}{\partial x^2} + \varepsilon(x, t). \tag{15}$$

The remainder term $\varepsilon(x, t)$ collects the higher-order derivatives

$$\varepsilon(x, t) = \frac{1}{\tau_c}\left[-\sum_{n=2}^{\infty} \frac{(\tau_c)^n}{n!}\frac{\partial^n C}{\partial t^n} + \sum_{n=2}^{\infty} \frac{(\lambda_c)^{2n}}{2n!}\frac{\partial^{2n} C}{\partial x^{2n}}\right]. \tag{16}$$

Note that in the process of deriving (15) from (14) no approximations were adopted. Accordingly, when the remainder term $\varepsilon(x, t)$ is kept, the "pseudo-diffusive" equation given by (15) remains entirely equivalent to the original Pearson model (14). Without the remainder term $\varepsilon(x)$, (15) becomes the classical biodiffusion model of bioturbation (Goldberg and Koide, 1962; Boudreau, 1986). We can now investigate under which conditions this remainder term can be neglected.

d. Spatial and temporal scales

At this point, our derivation differs from previous random-walk investigations (Wheatcroft *et al.,* 1990; Meysman *et al.,* 2003). To see this difference, we must first make a distinction between two different types of scaling, respectively associated with [1] the perspective of the moving particle, and [2] the perspective of the observer. The first perspective defines the so-called "process scales," which involve the characteristic time scale τ_c and the characteristic length scale λ_c. These quantities are inherent properties of the random walk process, and consequently, they do not depend on the experimental technique that is chosen to investigate this process. In the case of bioturbation, the quantities τ_c and λ_c are simply properties of the biological community that causes the sediment mixing: λ_c represents the characteristic length over which particles are displaced, and τ_c is the characteristic time interval between two bioturbation events. These parameters are tied to a certain biological community within a certain sediment environment and are not dependent on the experimental technique that is chosen to study bioturbation. Appendix A describes how these process scales τ_c and λ_c can be derived from the waiting time and jump length distribution respectively.

The second perspective defines the so-called "observational scales," which includes the observational length scale λ_{obs} and an observational time scale τ_{obs}. These observational parameters are not fixed for a given biological community, but depend on the experimental method that is chosen by the observer. For example, in a typical luminophore experiment, one follows the time-dependent down-mixing of a pulse of fluorescent particles over a time period of days and a depth interval of a couple of centimetres (e.g. Solan *et al.,* 2004; Maire *et al.,* 2007). However, the same sediment could also be examined by the ^{210}Pb method. In this case, the time-scale of observation would be tens of years rather than days, since ^{210}Pb has a half-life of 22.4 yr, and the penetration depth of the tracer would be a few tens of centimetres. Accordingly, the luminophore and ^{210}Pb methods result in different observational scales for the same bioturbation activity.

e. Long time limit: justification of the biodiffusion model

Based on the above arguments, one should clearly distinguish two sets of scales: the process scales τ_c and λ_c that are fixed and determined by the biology, and the observational scales τ_{obs} and λ_{obs} that are method-dependent and chosen by the observer. In classical derivations of the continuum limit (Murray, 1989; Wheatcroft *et al.,* 1990; Berg, 1993; Meysman *et al.,* 2003), the process scales are given a central role: one should take the limit of (15) so that τ_c and λ_c go to zero, but in such a way, that the ratio λ_c^2/τ_c neither becomes zero nor infinite. Formally, one then proves that in this limit, the remainder term provided by (16) vanishes, i.e., $\varepsilon(x, t) \mapsto 0$, and hence, (15) reduces to the classical biodiffusion model of bioturbation (Goldberg and Koide, 1962; Boudreau, 1986)

$$\frac{\partial C}{\partial t} = D_b \frac{\partial^2 C}{\partial x^2}. \tag{17}$$

The biodiffusion coefficient is then defined as

$$D_b = \lim_{\substack{\tau_c \to 0 \\ \lambda_c \to 0}} \left[\frac{1}{2} \frac{\lambda_c^2}{\tau_c} \right] \quad \text{with} \quad 0 < D_b < +\infty. \tag{18}$$

The limit operation (18) produces the desired result: one obtains the "macroscopic" biodiffusion model (17) as the asymptotic limit of the "microscopic" DSDT random walk (12). The underlying philosophy is nevertheless awkward: it implies that one should change the process scales! The quantities τ_c and λ_c are inherent properties of the bioturbation activity, and hence, their manipulation does not make much sense. The adaptation of τ_c and λ_c would imply that the ambient faunal community should be replaced by entirely new community, characterized by far smaller and more frequent particle displacements.

To avoid such a strange virtual replacement of the fauna, we propose an alternative limit operation, which focuses on the observational scales, rather than the process scales. Given N bioturbation events, the process and observational scales can be related via

$$\tau_{obs} = \tau_c N \tag{19}$$

$$\lambda_{obs} = \lambda_c \sqrt{N}. \tag{20}$$

For the moment, these scaling relations are introduced without further proof. Below, we will investigate in more detail how they can be justified. However, the link between the time scales (19) is intuitively clear: if τ_c is the characteristic time step between bioturbation events, then N events will be observed (on average) within the observational time frame τ_{obs}. The link between the length scales contained in (20) is also plausible. When the number of events increases, the tracer profile will show increasingly more spreading. As a result of this, the observer needs to expand the spatial scale of observation too. Eq. (20) states that the spreading (and hence the observational length scale λ_{obs}) does not increase

linearly, but scales with the square root of number of events N (a proof of this is given below). An important aspect of the scaling relations (19) and (20) is that the observational scales are coupled to the process scales via the number of bioturbation events N. This implies that τ_{obs} and λ_{obs} cannot be chosen independently. If one fixes τ_{obs} by choice of a certain experimental method, then λ_{obs} is determined, and vice versa. Up to now, this aspect has gone unnoticed in the literature on sedimentary particle mixing (we will return to this below).

The observational scales form the basis for the new asymptotic limit interpretation that is proposed here. When the number of bioturbation events increases, i.e., $N \mapsto +\infty$, both the observational scales will become large, i.e., $\tau_c \mapsto +\infty$ and $\lambda_c \mapsto +\infty$. Such a change of observational scales essentially requires that we change the experimental method used to study bioturbation, for example, by swapping from short-lived to long-lived isotopes as tracers. This is what we propose here. Rather than changing the macrofaunal community (as implied by the conventional limit procedure), we adapt the experimental method, so that process of bioturbation is studied over a larger spatial and temporal scales. As shown in Appendix C, one can prove that the remainder term vanishes when $N \mapsto +\infty$, i.e.,

$$\lim_{N\to\infty} [\varepsilon(x,t)] = \lim_{\substack{\tau_{obs}\to\infty \\ \lambda_{obs}\to\infty}} [\varepsilon(x,t)] = 0. \tag{21}$$

In this new limit operation, the ratio λ_c^2/τ_c in (15) will not change, since τ_c and λ_c are inherent properties of the bioturbation activity. Therefore, in the approach proposed here, the biodiffusion coefficient is defined as

$$D_b = \frac{1}{2}\frac{\lambda_c^2}{\tau_c}. \tag{22}$$

The important difference with the previous definition of biodiffusion coefficient, (18), is that the new definition in (22) does not involve a limit operation *for the biodiffusion coefficient.* The mixing intensity characterized by (22) comprises an inherent property of the bioturbation activity, solely defined in terms of the characteristic length scale λ_c over which particles are displaced, and the characteristic time interval τ_c between two bioturbation events. The mixing coefficient given by (22) can always be defined, and it remains valid for both small as well as for large values of N. Therefore, the pseudo-diffusive equation (15) can be rewritten in the form

$$\frac{\partial C}{\partial t} = D_b \frac{\partial^2 C}{\partial x^2} + \varepsilon(x,t). \tag{23}$$

This equation explains why there is no guarantee that biodiffusion model should work at short observation time scales (Meysman *et al.,* 2008b; Lecroart *et al.,* 2010). For small N, (23) should be applied with the remainder term. Only after a sufficient number of events, i.e. for large N, does the remainder term become small, and hence, Eq. (23) will reduce to the classical biodiffusion model (17) only for large N.

5. Discrete-Time Continuous-Space (DTCS) description

The constraint of a fixed jump distance underlying the DTDS model is often too stringent for particle movement in the natural environment. A clear example of this is the case of seed dispersal in higher plants (Levin *et al.,* 2003). Some seeds are deposited close to the parent plant, while others may be carried far away by various vectors such as wind, water and animals. Therefore, in models of seed dispersal the jump length is no longer fixed but described via a continuous dispersal curve, which functions as a probability distribution for the distance traveled by a seed (Kot *et al.,* 1996; Levin *et al.,* 2003). With regard to the frequency of seed dispersal events, the constant waiting time remains justified: seed dispersal by plants occurs in regular annual events. For the case of bioturbation, Meysman *et al.* (2003) also stressed that particles are displaced over different length scales in a bioturbation event, as the many different organisms present in the sediment display a wide variety of particle displacement mechanisms, e.g. burrowing, crawling, feeding, etc. Treating the jump length as a stochastic variable adds another stochastic degree of freedom (Fig. 2c).

a. Bioturbation as a Bachelier walk

Meysman *et al.* (2003) allow particles to jump to any location on the lattice during bioturbation, not only to the nearest neighbors. In this model, the waiting time T is deterministically fixed, but jump length L is turned into a stochastic variable. Accordingly, the resulting random walk model may be termed a *discrete-time continuous-space (DTCS) process.* In terms of the general stochastic model, the waiting time in the DTCS model remains $\Psi_T(\tau) = \delta(\tau - \tau_c)$ as in the Pearson walk (10), but the jump-length distribution $\Psi_L(\lambda)$ can now take any form. The redistribution of particles within the N-th bioturbation event is therefore described by the recursion relation

$$P_{N+1}(x) = \int_{-\infty}^{+\infty} \Psi_L(\lambda) P_N(x - \lambda) d\lambda \tag{24}$$

where $P_N(x)$ is the probability of finding a particle at position x after N steps. This DTCS process assumes that bioturbation events are independent, that they are always characterized by the same step length and waiting time distributions and that waiting and jumping behavior is independent. This results in the convolutive form of (24), which is typically referred to as Bachelier's equation (Hughes, 1995). In his doctoral thesis "La Théorie de la Spéculation," published in 1900, Bachelier proposed (24) as a random walk model for financial time series, and many decades later, Bachelier's ideas became the basis for modern theoretical finance. In the context of bioturbation, (24) has been used by Meile and Van Capellen (2005) and forms the basis of the so-called transition-matrix models of bioturbation (Jumars *et al.,* 1981; Foster, 1985; Trauth, 1998; Shull, 2001).

In a similar way as was done for the Pearson walk, we can now derive the diffusion equation from the Bachelier walk (24). Such a derivation was already presented in Meysman *et al.* (2003), but there, it was based on a Kramers-Moyal expansion in terms of raw moments. Here,

we show that this Kramers-Moyal procedure is incorrect, and that it should be replaced by a Gram-Charlier expansion in terms of cumulants (see Appendix B for a rigorous introduction to moments and cumulants). Neither raw nor centered moments are suitable statistics for the analysis of random walks, because they are not additive. Additivity requires that the statistic of the PDF of a sum of random variables should equal the sum of the statistics of the individual PDFs. This additivity is an important property because the position of a random walker is the sum of a set of jump vectors. Raw and centered moments are not additive, and therefore, they are not the proper statistics for the analysis of bioturbation by means of random walks. The sought after statistics are the cumulants K_n, which are additive, but are less familiar concepts than moments (see Appendix B for the calculation of cumulants).

b. Kramers-Moyal expansion

To show the deficiency in the continuum limit derivation of Meysman *et al.* (2003), we provide a short outline of their reasoning. In a similar way as done to arrive at (14), we can first replace the probability $P_N(x)$ by the concentration profile $C_N(x)$ by applying the Law of Large Numbers, and subsequently, implement $P(x, t) = P_N(x)$ at every time step $t = N\tau_c$, i.e., the continuum approximation. Bachelier's equation (24) thus transforms into the bioturbation model

$$C(x, t + \tau_c) = \int_{-\infty}^{+\infty} \Psi_L(\lambda) C(x - \lambda, t) d\lambda. \tag{25}$$

In the continuum limit derivation of Meysman *et al.* (2003), the left-hand side of (25) is expanded in a Taylor series about the time t. Subsequently, the higher order temporal derivatives are neglected, and (25) reduces to the form

$$\frac{\partial C}{\partial t} = \frac{1}{\tau_c} \int_{-\infty}^{+\infty} \Psi_L(\lambda)[C(x - \lambda, t) - C(x, t)] d\lambda. \tag{26}$$

Performing a Taylor series expansion of the concentration $C(x - \lambda, t)$, Eq. (26) can be recast into the form (Appendix C)

$$\frac{\partial C(x, t)}{\partial t} = \sum_{n=1}^{\infty} \frac{(-1)^n}{n!\tau_c} M_n \frac{\partial^n C}{\partial x^n}, \tag{27}$$

where M_n denote the raw moments of the jump-length distribution. Eq. (27) is referred to as a Kramers-Moyal moment expansion of Bachelier's equation (24) (Risken, 1996). The first and second raw moment can be cast in terms of the mean μ and variance σ^2 of the jump-length distribution, i.e., $M_1 = \mu$ and $M_2 = \sigma^2 + \mu^2$. Truncating the right-hand side of (27) after the second term, and introducing the bio-advective velocity $v_b = \mu/\tau_c$ and the biodiffusion coefficient $D_b = \sigma^2/2\tau_c$, one arrives at

$$\frac{\partial C}{\partial t} = -\nu_b \frac{\partial C}{\partial x} + (D_b + \mu\nu_b) \frac{\partial^2 C}{\partial x^2}. \tag{28}$$

This equation resembles the classical advection-diffusion model of bioturbation, but for the awkward $\mu\nu_b$ factor in front of the second-order derivative. The presence of this strange term indicates that the Kramers-Moyal approximation as in (27) is not a proper continuum limit of (25).

c. Gram-Charlier cumulant expansion

In the transition from (25) to (26), the higher-order temporal derivatives have all been discarded, thus introducing an important bias in the Kramers-Moyal approximation (27). This can be avoided by means of an alternative procedure, termed a Gram-Charlier cumulant expansion (see Appendix D). The Bachelier equation (24) is brought into the unbiased form

$$\frac{\partial C(x, t)}{\partial t} = \sum_{n=1}^{\infty} \frac{(-1)^n}{n!\tau_c} K_n[\Psi_L] \frac{\partial^n C}{\partial x^n}, \tag{29}$$

where $K_n[\Psi_L]$ represents the so-called n-th cumulant of the jump length distribution Ψ_L. Note the deceiving similarity between (27) and (29); the important difference is that the raw moments M_n in (27) have been replaced by the cumulants K_n in (29). Although this difference may seem to be only a mathematical nuance, it has in fact important implications for the mechanistic interpretation of the biodiffusion coefficient. We can define the bio-advective velocity and the biodiffusion coefficient respectively as

$$\nu_b \equiv \frac{K_1[\Psi_L]}{\tau_c} = \frac{\mu}{\tau_c} \tag{30}$$

$$D_b \equiv \frac{K_2[\Psi_L]}{2\tau_c} = \frac{\sigma^2}{2\tau_c}. \tag{31}$$

Using these terms, (29) can be rewritten in the "pseudo-diffusive" form

$$\frac{\partial C}{\partial t} = -\nu_b \frac{\partial C}{\partial x} + D_b \frac{\partial^2 C}{\partial x^2} + \varepsilon(x, t) \tag{32}$$

where the remainder term is defined as

$$\varepsilon(x, t) = \frac{1}{\tau_c} \sum_{n=3}^{\infty} \frac{(-1)^n}{n!} K_n[\Psi_L] \frac{\partial^n C}{\partial x^n}. \tag{33}$$

In contrast to (28), the "pseudo-diffusive" form of (32) has the proper form: it no longer features the awkward $\mu\nu_b$ factor in front of the second-order spatial derivative.

d. Asymptotic behavior after many bioturbation events

Similar to what was done above for the Pearson walk, one can prove that when the number of bioturbation events becomes large, i.e. $N \mapsto +\infty$, the remainder term in the pseudo-diffusive form of the Bachelier equation (32) will vanish Appendix E)

$$\lim_{N\to\infty} [\varepsilon(x,t)] = \lim_{\substack{\tau_{obs}\to\infty \\ \lambda_{obs}\to\infty}} [\varepsilon(x,t)] = 0. \tag{34}$$

Note that without the remainder term $\varepsilon(x)$, (32) becomes a classical advection-diffusion equation. When the remainder term $\varepsilon(x, t)$ is kept, the "pseudo-diffusive" (32) remains entirely equivalent to the original Bachelier equation in (24); this result occurs because in the process of deriving (32) from (24), no approximations or simplifications were adopted. As noted above, the limit operation in (34) requires that the observational scales from the observer's experimental technique should be sufficiently large. For small N, (32) should be applied with the remainder term $\varepsilon(x, t)$. For large N, the remainder term becomes small, and hence, (32) reduces to the classical biodiffusion model, i.e., (17).

6. Continuous-Time Continuous-Space (CTCS) description

The DTCS approach of the previous section treats both the direction and the distance of travel as stochastic, while keeping the frequency of events constant and deterministic. This approach seems suitable when modeling processes like seed dispersal, where dispersal events typically follow a regular annual pattern. However, in the case of particle movement due to bioturbation, there is no such inherent rhythm. The time between consecutive bioturbation events is variable by nature: the exact time when an organism will pass by and reshuffle the sediment is unpredictable. Therefore, Meysman *et al.* (2008a) recently proposed to also account for variability in the waiting time T of random walk descriptions of bioturbation. In this scenario, the direction, distance and frequency of jumping are all treated as stochastic variables (Fig. 2d).

a. Bioturbation as a Montroll-Weiss walk

Following the above classification, the resulting random walk may be termed a *continuous-time continuous-space (CTCS) process,* although in the statistics literature, the process is usually abbreviated to a continuous-time random walk (CTRW). The original development of CTCS models is tightly linked to the origin of the photocopying process, as traditional methods failed to describe the "anomalous" transport of charges in semiconductors (Montroll and Weiss, 1965; Metzler and Klafter, 2000). The CTCS random walk is not (yet) covered in treatments on biological dispersal (Murray, 1989; Okubo and Levin, 2001), but has generated a lot of attention in various physical sciences, such as ground water transport and chemical kinetics (Metzler and Klafter, 2000).

Recently, the CTCS was investigated as a model for bioturbation by Meysman *et al.* (2008a,b). The CTCS approach essentially provides the broadest application of the

stochastic model: both the jump-length distribution Ψ_L and the waiting-time distribution Ψ_T can now take any form. For a particle initially released at the origin, the probability $P(x, t)$ of finding such a particle at depth x after some time t is given by the renewal equation (Othmer *et al.,* 1988; Meysman *et al.,* 2008a),

$$P(x, t) = \delta(x)\left[1 - \int_0^t \Psi_T(\tau)d\tau\right] + \int_0^t \int_{-\infty}^{+\infty} \Psi_T(\tau)\Psi_L(\lambda)P(x - \lambda, t - \tau)d\lambda d\tau \quad (35)$$

where $\delta(x)$ is the Dirac delta function. This equation again assumes that bioturbation events are independent, characterized by the same step length and waiting time distributions, and that waiting and jumping behavior is independent. The first term on the right-hand side of (35) expresses the probability that a particle remains "unmoved" at the origin. The second (integral) term accounts for the "behavior" of the particle when it leaves its initial position. Note that the CTCS approach already provides a model description that is both continuous in time and in space. Accordingly, there is no continuum approximation step needed. To go from the "stochastic/single particle" level to the "deterministic/many particles" level, one only needs to invoke the law of large numbers (Feller, 1968). Given the initial concentration distribution of particles

$$C_0(x) = C(x, 0) \quad (36)$$

the concentration of particles at an arbitrary location x and time t is then expressed as

$$C(x, t) = C_0(x)\left[1 - \int_0^t \Psi_T(\tau)d\tau\right] + \int_0^t \int_{-\infty}^{\infty} \Psi_T(\tau)\Psi_L(\lambda)C(x - \lambda, t - \tau)d\lambda d\tau. \quad (37)$$

The initial value problem, as specified by (36) and (37), forms the complete statement of our CTRW model of bioturbation. Given a particular waiting time PDF $\Psi_T(\tau)$ and a jump length PDF $\Psi_L(\lambda)$, (37) will predict how the initial tracer profile $C_0(x)$ will evolve with time—see Meysman *et al.* (2008b) for details on the numerical solution procedure.

From the perspective of the CTRW model, a given bioturbation model is completely characterized by a particular combination of a waiting-time distribution $\Psi_T(\tau)$ and a jump-length distribution $\Psi_L(\lambda)$. The shape of these functions for a particular sediment setting will depend on the organisms that are present and the specific activities these organisms are displaying (e.g. deposit-feeding, burrowing). Collectively, we will refer to such a set of such conditions as a particular *bioturbation fingerprint.* Depending on the actual structure of the macrofaunal community (in terms of species composition, size, abundance and behavior), sediments can exhibit a range of bioturbation fingerprints, each characterized by a specific combination of Ψ_T and Ψ_L.

b. Asymptotic behavior after many bioturbation events

In a similar way as was done above for the Pearson and Bachelier process, we can now investigate the asymptotic behavior of (37). Again, the conclusion is that after a sufficiently

long time, i.e., when integrating a large number of bioturbation events, the response of the CTCS model will become diffusive and advective,

$$\frac{\partial C}{\partial t} = -v_b \frac{\partial C}{\partial x} + D_b \frac{\partial^2 C}{\partial x^2} + \varepsilon(x, t). \tag{38}$$

This asymptotic behavior applies a broad class of $\Psi_T(\tau)$ and $\Psi_L(\lambda)$ functions and is a well-known result from random walk theory (Hughes, 1995; Metzler and Klafter, 2000; a detailed proof is given in Appendix F). More specifically, one can prove that if the mean waiting time $\bar{\tau}$, as calculated via (A6) in Appendix A, the drift μ, as calculated via (A2), and the jump length variance σ^2, as calculated via (A4) are finite quantities, then for long times $t \sim \bar{\tau}$, the remainder term in (38) will vanish. The bio-advective velocity and the so-called biodiffusion coefficient are respectively defined as

$$v_b = \frac{\mu}{\bar{\tau}} \tag{39}$$

$$D_b = \frac{\sigma^2}{2\bar{\tau}}. \tag{40}$$

Eqs. (39)–(40) are very similar to (30)–(31). The subtle difference is that the fixed time scale τ_c is now replaced by the mean of the waiting-time distribution $\bar{\tau}$. Note that the advective-diffusive behavior for long times will not depend on the particular shape of the waiting-time and jump-length distributions. In other words, irrespective of the actual bioturbation regime that is in place, the long-time effect will always look like as a combination of advection and diffusive mixing.

7. Discussion

We have explored three different types of random walk models, which vary in the number of stochastic quantities that are incorporated: the Pearson (discrete space discrete time), Bachelier (continuous time discrete space) and Montroll-Weiss (continuous time continuous space) processes. Each time we have investigated the asymptotic behavior of these random walks. Based on this above analysis, we can now revisit the questions that were posed in the introduction.

[1] What are the assumptions underlying the biodiffusion model?

Our analysis reveals that there are a number of fundamental assumptions that should be met before particle mixing can be described via a truly diffusive model. These can be summarized as follows:

- *Particles are displaced independently.* Within a given bioturbation event, particles should not show collective behavior. Each particle should be displaced independently.

- *Successive bioturbation events are independent (Markov assumption).* Past events do not influence how a particle is displaced in the current mixing event. Each bioturbation event must act as an independent random event.
- *Sucessive bioturbation events are characterized by the same bioturbation fingerprint (Translational invariance of waiting time and step length distribution).* Strictly interpreted, this implies spatial and temporal homogeneity of mixing. In practice, this requires that the mixing mechanism should not exhibit abrupt changes in space and time.
- *A particle's jumping behavior is statistically independent from the waiting behavior.* The distance and direction over which a particle is displaced in a bioturbation event should not depend on how long this particle has waited before jumping, and vice versa.
- *The bioturbation fingerprint has finite statistics.* The waiting time distribution must have a finite mean and the step length distribution must have a finite variance.
- *Bioturbation events are sufficiently frequent, or observed over sufficiently long time scales (Frequency criterion).* Particles must experience a sufficient number of bioturbation events before mixing becomes diffusive.

Each of these conditions follows from assumptions that were adopted in the course of the derivations above. The requirement of independent displacement is necessary for the application of Law of Large Numbers—see discussion in connection to (13). The Markov assumption, the translation invariance and the statistical independence of jumping and waiting, are necessary to arrive at the convolutive form of the Bachelier equation (24) and the convolutive integral in the Montroll-Weiss equation (37). The finite statistics are required to bring the Bachelier and Montroll-Weiss equations in the pseudo-diffusive form, as in (32) and (38). The frequency criterion is needed for the remainder term $\varepsilon(x, t)$ in (32) and (38) to vanish in the limit for large N.

The above (long) list of constraints differs substantially from previous assessments of the conditions underlying the biodiffusion model. Typically, past works only mention three constraints, requiring that particle displacements should be [1] sufficiently small, [2] sufficiently frequent, and [3] randomly directed (Boudreau, 1986; Meysman *et al.,* 2003). Our analysis shows that this set of conditions is both inaccurate and incomplete. There are three important differences with previous assessments.

Firstly, directional randomness, also referred to as the symmetry criterion (Meysman *et al.,* 2003), does not feature in the list above. This is because it is not as essential as previously thought. When particle displacement is directionally nonrandom, this will simply introduce an bio-advective component in the resulting transport equation, hence resulting in an advection-diffusion equation—see (38). The presence of this advective component, however, does not fundamentally change the problem statement. The issues concerning the validity of the diffusion equation are exactly the same as those of the advection-diffusion equation. The crucial issue is whether, when and why the pseudo-(advection-) diffusion equation given by (32) or (38) can be used without the remainder

term $\varepsilon(x, t)$? Therefore, directional randomness is not a crucial constraint with respect to the applicability of the biodiffusion model. Also note that when asymmetric mixing occurs (generating bio-advection), the mixing process cannot be the same throughout the sediment. Downward asymmetric mixing in one depth zone must always be compensated by upward asymmetric mixing in another depth horizon (see the example of conveyor-belt mixing below). The whole sediment column cannot be subject to the same bio-advective velocity. If this would be the case, then the sediment would move as a whole, which is not the case. Bioturbated sediments as a whole stay nicely in place; they are just continuously turned upside down.

A second point is that the length scale criterion (small particle displacements) and the frequency criterion (sufficiently frequent displacements) are traditionally seen as two independent constraints, e.g. Meysman *et al.* (2003). Here, we show that spatial and temporal criteria are not separate conditions, but that they are tightly linked through the number of bioturbation events N—see (19) and (20). Given a sufficient number of bioturbation events and provided that all other conditions are fulfilled, any mixing regime will eventually become diffusive. To observe more mixing events, one has to increase the observational time scale. Yet, as an unavoidable side effect, the spatial scale over which one observes the particles will automatically increase as well. In more mixing events, the particles will also spread more, and so the step length becomes smaller compared to the overall size of the domain under observation, which scales with the square root of N—see (20). Because of this tight coupling, the single frequency criterion here replaces the previous two requirements that particle displacement should that be sufficiently small and sufficiently frequent. Particles should experience a sufficiently high number of bioturbation events, before the resulting tracer mixing can be interpreted with a biodiffusion model.

The third major difference is that we list five extra constraints on particle displacement, before it can be described via a diffusive mixing model. As further detailed below, these conditions are crucial to understand why certain bioturbation activities result in tracer profiles that cannot be described by the common biodiffusion model.

[2] How to account for biological variability in bioturbation models?

Simple random walk models of bioturbation have been criticized for their lack of biological realism, as they adopt a fixed jump length and fixed jumping frequency. Sediments are typically inhabited by a diverse community of sediment-dwelling macrofauna. These organisms disturb the sediment differently depending on their specific feeding type, mobility, and life cycle (Cadee, 2001; Solan and Wigham, 2005). Accordingly, sediment particles will experience different types of movement in consecutive bioturbation events. A clear issue in bioturbation modeling is how this biological variability can be incorporated into particle dispersal models (Jumars *et al.,* 1981; Boudreau and Imboden, 1987; Shull, 2001; Meysman *et al.,* 2003).

In the past, a distinction has been made between so-called "local" mixing where particles are displaced to nearest neighborhood sites, and "nonlocal" mixing that allow long-range mass transfer between spatially separated layers within the sediment (Jumars *et al.,* 1981;

Boudreau and Imboden, 1987; Francois *et al.,* 2001; Shull, 2001; Meysman *et al.,* 2003). Our analysis shows that this classification appears to be less fundamental than previously thought. In the traditional view, the Pearson random walk (12) would be called "local" mixing, where both the Bachelier model (24) and the Montroll-Weiss model (37) would qualify as "nonlocal" mixing. However, as we clearly show, all three models will exhibit diffusive mixing over long times. So in terms of their mixing properties, the Pearson (12), Bachelier (24) and Montroll-Weiss (37) models are not fundamentally different.

Our present analysis clarifies how biological variability can be incorporated into bioturbation models. Two source types of variability are distinguished, which relate to the distances over which particles are displaced (the jumping behavior), and to the time a particle rests between bioturbation events (the waiting behavior). By considering the waiting time and jump length as either stochastic or deterministic, one arrives at different random-walk models. The most general description is the Montroll-Weiss random walk, which leads to the concept of a bioturbation fingerprint (Meysman *et al.,* 2008a). In this model, particle displacement is described by two separate probability distributions, the waiting-time and the jump-length distributions. A challenge in future studies will be to determine the bioturbation fingerprint of various macrofaunal communities under natural conditions.

[3] Can we provide an explicit link between biological activity and the biodiffusion coefficient?

Based on dimensional analysis, it is clear that the biodiffusion coefficient D_b can be decomposed as the square of a characteristic length scale λ_c divided by a time scale τ_c (Boudreau, 1989; Wheatcroft *et al.,* 1990; Swift *et al.,* 1996). A crucial question is how the parameters λ_c and τ_c should be calculated and interpreted. Eq. (40) provides the sought-after solution, and determines how τ_c and λ_c can be derived from the bioturbation fingerprint characterizing the bioturbation activity of a macrofaunal community. This analysis shows that the "natural" length and time scale of bioturbation are respectively defined as

$$\lambda_c = \sqrt{\sigma^2} \tag{41}$$

$$\tau_c = \bar{\tau} \tag{42}$$

where $\bar{\tau}$ is the mean waiting time between bioturbation events, i.e., the first raw moment of the waiting-time distribution, and σ^2 is the variance of the jump lengths, i.e., second central moment of the jump-length distribution. A striking observation is that the characteristic scales depend on a peculiar mix of raw and central moment statistics. Our detailed investigation shows that the cumulants (and not the moments) are the proper statistics for the analysis of bioturbation by means of random walks. This is essentially because cumulants are additive quantities, and a random walk is basically an addition of consecutive jump vectors. The first cumulant equals the mean or first raw moment (defining τ_c), while the second cumulant equals the variance or second central moment (defining λ_c).

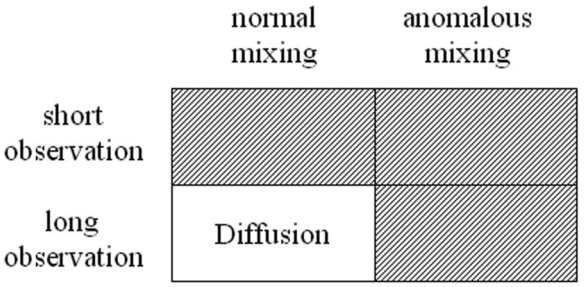

Figure 3. Schematic overview of the conditions that lead to diffusive mixing. Two factors are crucial: the inherent nature of the mixing activity, i.e, whether it is "normal" or "anomalous," (this depends on the statistics of the waiting time and step length disribution) and the time scale over which the mixing process is observed, i.e., short or long time scales. Only normal mixing observed over sufficiently long time scales leads to diffusive mixing.

The higher cumulants of the jump-length and waiting-time distributions influence particle dispersal at short times (nondiffusive mixing regime), but vanish at long times (diffusive mixing regime).

[4] What's the relation between the biodiffusion model and more sophisticated models?

In the literature on particle dispersal in sediments and soils, there is a certain misunderstanding about the position of the biodiffusion model. Often, there is a polarization, where the biodiffusion model is positioned against more complex "nonlocal" approaches (Jumars *et al.,* 1981; Francois *et al.,* 2001; Shull, 2001; Meysman *et al.,* 2003). This creates the impression that the biodiffusion model is an entirely independent and unrelated description of bioturbation. Here, we again show that this is a major misconception, and that the biodiffusion is in fact tightly related to more complex approaches. Both the Bachelier model (24) and the Montroll-Weiss model (37) qualify as "nonlocal," but these models will exhibit diffusive mixing over long times. Rather than "local" and "nonlocal," we propose a far more fundamental distinction between faunal mixing activities, based on whether the resulting transport will become diffusive in the long term. This leads to two basic types of mixing with associated models.

A first class of faunal mixing activities and associated bioturbation models can be classified as "normal" mixing (Fig. 3). These models may show a nondiffusive response over the short term, but over long terms, they eventually converge to diffusive mixing. Both the "nonlocal" Bachelier (24) and Montroll-Weiss (37) models belong to this group, provided that the waiting time distribution has a finite mean and the step length distribution has a finite variance. These models are not inherently different from the biodiffusion model. They are simply capable of "observing" the mixing process over small enough time scales, where the limit approximation underlying the biodiffusion model is not yet valid. At small time scales, the tracer profiles produced by the Montroll-Weiss CTRW model differ from the biodiffusion model, yet at long times, the simulation output becomes indistinguishable—see Figure 5 in Meysman *et al.* (2008a). Another example is the Telegraph model,

which was proposed by Boudreau (1989) as an alternative to the biodiffusion model. In essence, this telegraph models assumes that steps are correlated, i.e., the Markov assumption is violated at short time scales (Meysman *et al.,* 2008a). Yet, at longer time scales, the telegraph solutions converge to those of the biodiffusion model (Boudreau, 1989). Accordingly, the question whether a more complex model is different from the biodiffusion model, is not simply a matter of inherent model characteristics, but also a matter of time scale. Exactly the same type of bioturbation activity can be perceived as "diffusive" and "nondiffusive," depending on whether it is observed over long and short time scales, respectively (e.g. by long-lived versus short-lived radionuclides).

A second class of faunal mixing activities and associated bioturbation models can be called "anomalous" mixing (Fig. 3). This group contains models that are truly different from the biodiffusion model, as they do not show diffusive behavior at long observation times. Such "anomalous" behavior must be caused by the violation of one of the criteria listed above (note however that a violation need not necessarily result in anomalous mixing). Two cases are particularly relevant to bioturbation. A first situation occurs when the bioturbation fingerprint displays infinite statistics, i.e., when either the mean of the waiting time distribution or the variance of the step-length distribution are infinite. These conditions give rise to subdiffusion and superdiffusion at long times (see Meysman *et al.,* 2008a for detailed account). Such anomalous diffusion has received a lot of attention in the physical literature, but the relevance for bioturbational mixing remains unclear, and needs further investigation (see Meysman *et al.,* 2008a for a more detailed discussion).

For bioturbation research, the most important deviation from "normal mixing" occurs when the mixing activity is strongly nonhomogeneous. An important example is head-down deposit-feeding, where the step-length distribution abruptly changes at the feeding depth of the deposit-feeding organism (Fig. 4). Sediments dominated by head-down deposit feeders often show subsurface tracer peaks, and such peaks cannot be generated by a biodiffusion model. To still model such tracer profiles, "nonlocal" conveyor-belt mixing models have been proposed that simulate tracer transport by head-down deposit feeders (Fisher *et al.,* 1980; Robbins, 1986; Rice, 1986; Delmotte *et al.,* 2007). These models typically include sediment ingestion at depth, with the ingested material subsequently deposited at the sediment-water interface. This creates a conveyor belt mechanism, resulting in an advection of sediment from the sediment-water interface downward to the feeding depth. In the framework presented here, this conveyor belt transport causes a strong spatial dependence and asymmetry in the probability distribution functions describing particle transport. At the feeding depth, one has an abrupt change in the shape of the step length distribution (Fig. 4).

Accordingly, one of the above criteria (the translational invariance of step length distribution) is strongly violated. As a result, conveyor belt models will not show diffusive behavior at long times. Conveyor-belt mixing models belong to the "anomalous" mixing category, not because they include "nonlocal" transport between distant sediment layers,

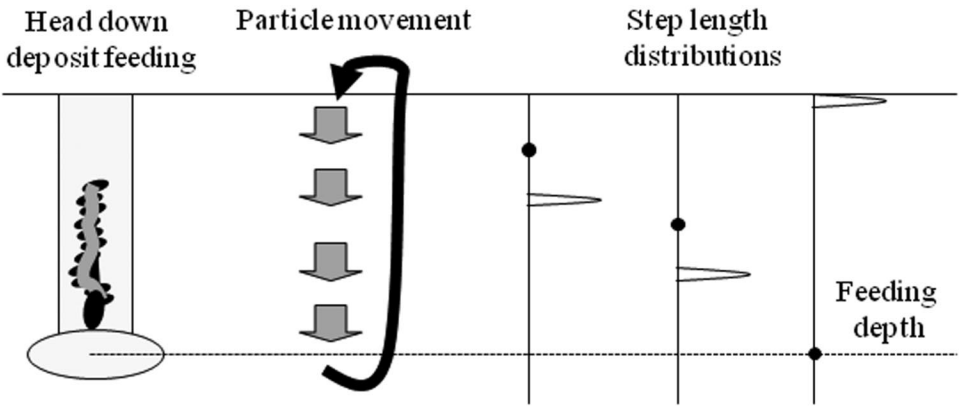

Figure 4. A prominent example of nondiffusive mixing: head-down deposit feeding leading to conveyor-belt transport of particles. The prime reason for the nondiffusive charter of conveyor-belt mixing is that violates the criterion of translational invariance. Conveyor-belt mixing causes a strong spatial dependence of the step length distribution that describes particle mixing. The step length distribution is shown at three depths in the sediment (as indicated by the black dots). At the feeding depth, the step length distribution changes abruptly in shape.

but because this transport is highly asymmetric (only from depth to the sediment-water interface).

[5] Is the "diffusive" character of down-core tracer profiles really surprising?

In both field and laboratory tracer studies, a fair proportion of the data appear "diffusive," i.e., tracer profiles that can be fitted adequately with suitable solutions of the classical diffusion equation. Our model analysis shows that such "diffusive" data are not surprising at all. After a sufficiently "long" time, the three random walk models that are analyzed here can all converge to the diffusion equation. In other words, when the observational time scale is large enough (i.e. after a sufficient number of bioturbation events), the response of the Pearson, Bachelier and Montroll-Weiss models cannot be distinguished from that of the asymptotic diffusion model. In essence, this is simply a consequence of the Central Limit Theorem. This also explains why the diffusion equation takes such a central role in a wide variety of natural sciences, and hence, also in the study of bioturbation. The critical condition is the frequency criterion: the mixing must be observed over a sufficiently long time scale, so that enough bioturbation events have taken place.

Based on this, one would expect diffusive mixing be the norm rather than the exception, particularly for long-lived tracer experiments. Nonetheless, it is important to realize that the random-walk models examined here contain simplifying assumptions (statistical independence of jumping and waiting, temporal and spatial homogeneity, finite statistics). When these assumptions are not met, the asymptotic state of diffusive mixing may not be reached. As noted above, a deviation from diffusion can be expected when the mixing activity is strongly nonhomogeneous. A most prominent example of this is the mixing caused by head-down deposit-feeding (Fisher *et al.,* 1980; Robbins, 1986; Rice, 1986;

Delmotte *et al.,* 2007). Further studies are warranted on the asymptotic behavior of nonhomogeneous bioturbation fingerprints.

[6] When can we apply the biodiffusion model, and when should we employ more sophisticated models?

When applying bioturbation models to tracer profiles, one should in essence answer two questions (Fig. 3). The first task is to decide whether one should use an "anomalous" mixing model or "normal" mixing model. This intrinsically depends on the nature of the bioturbation activities at the site. Some activities can be cast into the "normal" framework, other activities such as head-down deposit feeding (see discussion above) will violate the conditions for "normal" mixing. Secondly, if one can use a "normal" mixing model, one should look at the time scale over which the mixing is observed. This time scale depends on the tracer that is employed (e.g. long-lived radiotracers versus short-lived radiotracers). Particle dispersal only becomes truly diffusive for sufficiently "long" times. Accordingly, tracers should be sufficiently long-lived before one can employ the biodiffusion model to extract a Db value from tracer profiles. Over short-time scales (depth profiles of short-lived radiotracers, short time pulse chase experiments with conservative tracers), one needs more sophisticated "normal" mixing models, like the CTRW model (Meysman *et al.,* 2008a).

This immediately begs the question as to what is "sufficiently long" (i.e. when is the frequency criterion met?). Our analysis shows that this "diffusive limit" has been misinterpreted in past treatments. This is because of a mix-up of the two different time scales that are involved in particle dispersal. On the one hand, one should distinguish the process time scale τ_c, which is determined by the biota, and represents the mean time interval between two bioturbation events. On the other hand, one has the observational time scale τ_{obs}, which is chosen by the biologist through the experimental method that is selected to study bioturbation (e.g. by using long-lived versus short-lived radionuclides). Diffusive mixing can be expected when the observational time scale τ_{obs} sufficiently exceeds the process time scale τ_c. Recent theoretical investigations indicate that τ_{obs} should be at least 10 to 20 times larger than the average waiting time $\bar{\tau} = \tau_c$ (Reed *et al.,* 2006, 2007; Maire *et al.,* 2007; Meysman *et al.,* 2008a). In other words, by selecting the proper experimental method, and hence adapting τ_{obs} to a large enough value, one can expect to collect "diffusive" data profiles, which can be well fitted with the biodiffusion model. However, if one selects an experimental method with a too small observational time scale τ_{obs}, one may expect that tracer profiles will differ from classical diffusive profiles, and so the analysis of such data will generally require more complex formulations like the CTRW model (Meysman *et al.,* 2008a).

Acknowledgments. This research was supported by grants from the Research Foundation—WO Odysseus grant to FJRM), the Netherlands Organization for Scientific Research (VIDI to FJRM), and Natural Sciences and Engineering Research Council of Canada and US Office of Naval Research (to BPB). This is publication 5004 of the Netherlands Institute of Ecology (NIOO-KNAW) and contributes to the Darwin Institute for Biogeosciences. We thank two anonymous reviewers for their constructive and accurate comments which greatly helped to improve the paper.

APPENDIX A

Length and time scales of bioturbation

As known from statistical theory (Feller, 1968), the general way to define the characteristic scales of a probability distribution $\Psi(u)$ is to use a certain weighing function $f(u)$, and calculate the expected value $\langle f(u) \rangle$ as

$$\langle f(u) \rangle \equiv \int_{-\infty}^{\infty} f(u)\Psi(u)du. \tag{A1}$$

Based on the above expression, many different "averages" can be calculated for $\Psi(u)$, depending on the weighing function $f(u)$ that is used. Therefore, the use of the term "average" with no further specification is problematic, and hence, we need a clear procedure how to derive the characteristic length scale λ_c and characteristic time interval τ_c for particular waiting time Ψ_T and jump length Ψ_L distributions. The mean of the jump-length distribution is usually referred to as the "drift" μ and represents the net particle displacement

$$\mu = \int_{-\infty}^{\infty} \lambda\Psi_L(\lambda)d\lambda. \tag{A2}$$

To obtain a nonvanishing drift $\mu \neq 0$, either the jump-distance distribution must be dependent on the direction (i.e., nonisotropy) or the jump-angle distribution should be nonuniform (i.e., directionality so that $p \neq 1/2$). Because μ vanishes in the case of symmetric mixing, it is not a suitable candidate for the characteristic length scale λ_c. However, using the drift, one can define a series of length scales via the higher moments of the step length distribution

$$\lambda_{c,n} = \sqrt{\langle |L - \mu|^n \rangle} \quad \text{with} \quad \langle |L - \mu|^n \rangle = \int_{-\infty}^{\infty} |\lambda - \mu|^n \Psi_L(\lambda)d\lambda. \tag{A3}$$

Due to the presence of the n-th power under the integral in (A3), the influence of long-range displacements will become more dominant in the associated length scale λ_c with increasing n. The question then is what n corresponds to a certain "natural" or true characteristic length scale? There is no *a priori* reason why a particular value for n in (A3) should be preferable over all other length scales. Yet, as shown in the main text, the variance or second central moment is of special importance,

$$\sigma^2 = \int_{-\infty}^{\infty} [\lambda - \mu]^2 \Psi_L(\lambda)dL. \tag{A4}$$

A similar series of time scales can be defined using the waiting time distribution

$$\tau_{c,n} = \sqrt{\langle T^n \rangle} \quad \text{with} \quad \langle T^n \rangle = \int_0^\infty \tau^n \Psi_T(\tau) d\tau. \tag{A5}$$

Again, there is no a priori reason why a particular value for n in (A3) should be preferable over all other time scales. Nonetheless, as shown in the main text, the first moment or the mean $\bar{\tau}$ of the waiting-time distribution will be of special importance

$$\bar{\tau} = \int_0^\infty \tau \Psi_T(\tau) d\tau. \tag{A6}$$

In summary, we are confronted with a problematic arbitrariness in the definition of the process scales λ_c and τ_c that characterize bioturbation. There are multiple ways in which λ_c and τ_c can be extracted from a particular set of waiting-time and the jump-length distributions. The question then is whether there are any particular values of λ_c and τ_c that are preferential over all other "averages" from a theoretical point of view. The answer is yes. As shown in the main text, the mean of the waiting time distribution and the variance of the step length distribution are the "natural" length and time scales of bioturbation.

APPENDIX B

Moments and cumulants

Different distributions can be compared and classified by means of so-called descriptive statistics; i.e., quantities that adequately summarize the information contained in the given a probability density function. Well-known statistics from introductory textbooks on probability theory are the raw and centered moments, which are respectively defined as

$$M_n \equiv \langle u^n \rangle = \int_{-\infty}^\infty u^n \Psi(u) du \tag{A7}$$

$$\bar{M}_n \equiv \langle (u - M_1)^n \rangle = \int_{-\infty}^\infty (u - M_1)^n \Psi(u) du. \tag{A8}$$

The raw moments take the origin as the reference point, while the centered moments use the first moment M_1 as the reference. Cumulants cannot be calculated directly using an explicit formula like (A7) or (A8). Instead, the n-th cumulant K_n must be obtained by nonlinear combination of lower-order moments following a quite intricate procedure based upon Fourier transformations (see below). The cumulants up until $n = 4$ have been designated special names, and their relation with the corresponding raw and centered moments is given by

Mean	$K_1 = M_1$
Variance	$K_2 = \bar{M}_2 = M_2 - M_1^2$
Skewness	$K_3 = \bar{M}_3 = M_3 - 3M_1M_2 + 2\{M_1\}^3$
Kurtosis	$K_4 = \bar{M}_4 - 3\{\bar{M}_2\}^2 = M_4 - 3\{M_2\}^2 - 4M_1M_3 + 12\{M_1\}^2M_2 - 6\{M_1\}^4.$

As can be seen, the first cumulant K_1 is simply the mean or first raw moment of the PDF. Similarly, the second cumulant K_2 equals the variance (or second centered moment). The third cumulant is also identical to the third centered moment, but the fourth cumulant differs from the fourth centered moment.

An alternative way to derive the raw moments M_n is from the *moment-generating function*

$$\hat{\Psi}(\xi) \equiv \langle \exp(i\xi x) \rangle = \int_{-\infty}^{\infty} \Psi(x) \exp(i\xi x) dx \tag{A9}$$

which is simply the Fourier transform of the probability density function $\Psi(x)$. By using a Taylor expansion around the origin, one can readily see that the *moment-generating function* (A9) conveniently encodes the raw moments, i.e.,

$$\hat{\Psi}(\xi) = 1 + \sum_{n=1}^{\infty} \frac{(-i)^n}{n!} M_n \xi^n = 1 - iM_1\xi + \frac{1}{2} M_2 \xi^2 \ldots \tag{A10}$$

As a result, the moments can be generated as

$$M_n = i^{-n} \left. \frac{d^n \hat{\Psi}(\xi)}{d\xi^n} \right|_{\xi=0}. \tag{A11}$$

The cumulant-generating function is defined as the natural logarithm of the moment-generating function.

$$\psi(\xi) = \ln [\hat{\Psi}(\xi)]. \tag{A12}$$

Expanding this function in a Taylor series around the origin, one obtains

$$\ln [\hat{\Psi}(\xi)] = \sum_{n=1}^{\infty} \frac{(-i)^n}{n!} K_n \xi^n = -iK_1\xi + \frac{1}{2} K_2 \xi^2 \ldots \tag{A13}$$

As a result, the cumulant of order n is defined as

$$K_n = i^{-n} \left. \frac{d^n \ln[\hat{\Psi}(\xi)]}{d\xi^n} \right|_{\xi=0}. \tag{A14}$$

It follows from relations (A10) and (A13) that the first n cumulants can be expressed in terms of the first n moments.

APPENDIX C

Long time limit of a Pearson walk

The starting point of our derivation is the recursion relation (A14)

$$C(x, t + \tau_c) = \frac{1}{2}[C(x - \lambda_c, t) + C(x + \lambda_c, t)]. \tag{A15}$$

The probabilities on both sides of (A15) can be expanded in a Taylor series as

$$C(x, t + \tau_c) = C(x, t) + \sum_{n=2}^{\infty} \frac{(\tau_c)^n}{n!} \frac{\partial^n C}{\partial t^n} \tag{A16}$$

$$C(x \pm \lambda_c, t) = C(x, t) + \sum_{n=2}^{\infty} \frac{(\pm\lambda_c)^n}{n!} \frac{\partial^n C}{\partial x^n}. \tag{A17}$$

Upon substitution of (A16) and (A17) into(A15), we obtain

$$\frac{\partial C}{\partial t} = \frac{\lambda_c^2}{2\tau_c} \frac{\partial^2 C}{\partial x^2} + \frac{1}{\tau_c}\left[- \sum_{n=2}^{\infty} \frac{(\tau_c)^n}{n!} \frac{\partial^n C}{\partial t^n} + \sum_{n=2}^{\infty} \frac{(\lambda_c)^{2n}}{2n!} \frac{\partial^{2n} C}{\partial x^{2n}} \right]. \tag{A18}$$

We can now examine the behavior of the remainder term in (A18) after a sufficient amount of bioturbation events, i.e., large N. For this, it is useful to bring (A15) in a dimensionless form. To this end, one can use the time scale τ_{obs} and length scale λ_{obs} over which the random walk is observed. By means of the dimensionless variables $\tilde{x} = x/\lambda_{obs}$, and $\tilde{t} = t/\tau_{obs}$, (A15) can be brought into the dimensionless form

$$\frac{\partial C}{\partial \tilde{t}} = \frac{\tau_{obs}}{\{\lambda_{obs}\}^2} \frac{\lambda_c^2}{2\tau_c} \frac{\partial^2 C}{\partial \tilde{x}^2} + \frac{1}{\tau_c}\left[- \sum_{n=2}^{\infty} \frac{1}{n!} \left(\frac{\tau_c}{\tau_{obs}}\right)^n \frac{\partial^n C}{\partial \tilde{t}^n} + \sum_{n=2}^{\infty} \frac{1}{2n!} \left(\frac{\lambda_c}{\lambda_{obs}}\right)^{2n} \frac{\partial^{2n} C}{\partial \tilde{x}^{2n}} \right]. \tag{A19}$$

The crucial task is now to find appropriate expressions for the observational time scale τ_{obs} and the length scale λ_{obs}. To this end, use the scaling relations:

$$\tau_{obs} = \tau_c N \tag{A20}$$

$$\lambda_{obs} = \lambda_c \sqrt{N}. \tag{A21}$$

Implementing these scaling relations, (A20) and (A21), into(A19), we arrive at

$$\frac{\partial C}{\partial \tilde{t}} = \frac{1}{2} \frac{\partial^2 C}{\partial \tilde{x}^2} + \frac{1}{\tau_c}\left(\frac{1}{N}\right)^n \left[\sum_{n=2}^{\infty} \frac{1}{n!} \frac{\partial^n C}{\partial \tilde{t}^n} + \sum_{n=2}^{\infty} \frac{1}{2n!} \frac{\partial^{2n} C}{\partial \tilde{x}^{2n}} \right]. \tag{A22}$$

In this asymptotic limit for $N \mapsto \infty$, i.e. after a large number of bioturbation events, Eq. (A22) reduces to

$$\frac{\partial C}{\partial \tilde{t}} = \frac{1}{2} \frac{\partial^2 C}{\partial \tilde{x}^2} . \tag{A23}$$

and hence, the remainder term vanishes, i.e., $\varepsilon(x, t) \mapsto 0$ for $N \mapsto \infty$.

APPENDIX D

Kramers-Moyal moment expansion

To obtain the continuum limit of Bachelier's equation (25) we can expand the concentration profile $C_N(x - \lambda)$ under the integral on the right-hand side in a Taylor series at the point x, i.e.,

$$C_N(x - \lambda) = C_N(x) + \sum_{n=1}^{\infty} \frac{(-1)^n}{n!} \lambda^n \frac{\partial^n C}{\partial x^n} . \tag{A24}$$

Upon back substitution into (25) and dividing by the waiting time τ_c, we obtain the equivalent formulation

$$\frac{C_{N+1}(x) - C_N(x, t)}{\tau_c} = \sum_{n=1}^{\infty} \frac{(-1)^n}{n! \tau_c} M_n(x) \frac{\partial^n C}{\partial x^n} \tag{A25}$$

where the "raw" moments M_n of the jump-length distribution are defined through (A7).

Eq. (A25) is still a difference equation, and not a differential equation. Introduce the $C(x, t)$ as the continuous-time approximation of $C_N(x)$, so that $C(x, N\bar{\tau}) = C_N(x)$ holds at every step $t = N\bar{\tau}$, we find that

$$\frac{C(x, t + \tau_c) - C(x, t)}{\tau_c} = \sum_{n=1}^{\infty} \frac{(-1)^n}{n! \tau_c} M_n(x) \frac{\partial^n C}{\partial x^n} . \tag{A26}$$

The left-hand side of (A25) strongly resembles the time derivative of $C(x, t)$. It is therefore tempting to approximate (A26) as

$$\frac{\partial C(x, t)}{\partial t} = \sum_{n=1}^{\infty} \frac{(-1)^n}{n! \tau_c} M_n(x) \frac{\partial^n C}{\partial x^n} . \tag{A27}$$

Eq. (A27) is referred to as the "Kramers-Moyal" moment expansion (Risken, 1996) in which, the raw moments M_n feature as the crucial statistics.

APPENDIX E

Gram-Charlier cumulant expansion

In the transition from (A26) to (A27) the higher-order temporal derivatives have been discarded, thus introducing an important bias in the Kramers-Moyal approximation (A27). In order to keep higher-order temporal derivatives, we can expand $C(x, t + \tau_c)$ in a Taylor series around t, so that equation (A26) becomes

$$\frac{\partial C}{\partial t} + \sum_{n=2}^{\infty} \frac{\tau_c^{n-1}}{n!} \frac{\partial^n C}{\partial t^n} = \sum_{n=1}^{\infty} \frac{(-1)^n}{n!\tau_c} M_n(x) \frac{\partial^n C}{\partial x^n}. \tag{A28}$$

In a subsequent step, we can use a recursive substitution procedure, where equation (A28) is multiplied by the operator $(\tau_c/2)\partial/\partial t$, so that

$$\frac{\tau_c}{2} \frac{\partial^2 C}{\partial t^2} + \sum_{n=2}^{\infty} \frac{\tau_c^{n+1}}{n!2} \frac{\partial^{n+1} C}{\partial t^{n+1}} = \sum_{n=1}^{\infty} \frac{(-1)^n}{n!2} M_n(x) \frac{\partial^n}{\partial x^n} \left[\frac{\partial C}{\partial t} \right]. \tag{A29}$$

The next step is to substitute $\partial C/\partial t$ from Eq. (A28) into (A29) to obtain

$$\frac{\tau_c}{2} \frac{\partial^2 C}{\partial t^2} + \sum_{n=2}^{\infty} \frac{\tau_c^{n+1}}{n!2} \frac{\partial^{n+1} C}{\partial t^{n+1}} = \sum_{n=1}^{\infty} \frac{(-1)^n}{n!2} M_n(x) \frac{\partial^n}{\partial x^n} \left[\sum_{n=1}^{\infty} \frac{(-1)^n}{n!\tau_c} M_n(x) \frac{\partial^n C}{\partial x^n} - \sum_{n=2}^{\infty} \frac{\tau_c^{n-1}}{n!} \frac{\partial^n C}{\partial t^n} \right] \tag{A30}$$

which can be rewritten as

$$\frac{\tau_c}{2} \frac{\partial^2 C}{\partial t^2} = \frac{\{M_1^2\}}{2\tau_c} \frac{\partial^2 C}{\partial x^2} + \frac{\{M_1^3 - 2M_1 M_2\}}{4\tau_c} \frac{\partial^3 C}{\partial x^3} - \frac{\{\tau_c\}^2}{4} \frac{\partial^3 C}{\partial t^3} + \mathrm{O}\left(\frac{\partial^4 C}{\partial x^4}, \frac{\partial^4 C}{\partial t^2} \right). \tag{A31}$$

We can now multiply this expression again with the operator $(\tau_c/2)\partial/\partial t$, to obtain

$$\frac{\tau_c^2}{4} \frac{\partial^3 C}{\partial t^2} = -\frac{M_1^3}{4\tau_c} \frac{\partial^3 C}{\partial x^3} + \mathrm{O}\left(\frac{\partial^4 C}{\partial x^4}, \frac{\partial^4 C}{\partial t^2} \right). \tag{A32}$$

The above procedure of (A29)–(A32) expresses the temporal derivative of order n each time in terms of spatial derivatives and the temporal of order $\geq n + 1$. This way the temporal derivatives can be systematically removed from the expansion (A28). Upon substitution of (A31) and (A32) into the original expansion(A28), we finally obtain

$$\frac{\partial C}{\partial t} = -\frac{M_1}{\tau_c} \frac{\partial C}{\partial x} + \frac{\{M_2 - M_1^2\}}{2\tau_c} \frac{\partial^2 C}{\partial x^2} - \frac{\{M_3 - 3M_1 M_2 + 2M_1^3\}}{6\tau_c} \frac{\partial^3 C}{\partial x^3} + \mathrm{O}\left(\frac{\partial^4 C}{\partial x^4}, \frac{\partial^4 C}{\partial t^2} \right). \tag{A33}$$

The combinations of raw moments in (A33) form exactly the cumulants as defined in Appendix B, and so we obtain,

$$\frac{\partial C}{\partial t} = -\frac{K_1}{1!\tau_c}\frac{\partial C}{\partial x} + \frac{K_2}{2!\tau_c}\frac{\partial^2 C}{\partial x^2} - \frac{K_2}{3!\tau_c}\frac{\partial^3 C}{\partial x^3} + \mathrm{O}\left(\frac{\partial^4 C}{\partial x^4}, \frac{\partial^4 C}{\partial t^2}\right). \tag{A34}$$

Generalizing the formula, (A33), the expansion can be brought in the so-called Gram-Charlier form, which now features the cumulants, instead of the raw moments as the Kramers-Moyall form (A27),

$$\frac{\partial C(x, t)}{\partial t} = \sum_{n=1}^{\infty} \frac{(-1)^n}{n!\tau_c} K_n(x) \frac{\partial^n C}{\partial x^n}. \tag{A35}$$

APPENDIX F

Long-time behavior of the Bachelier walk

We want now to examine the behavior of the remainder term (A38) after a sufficient amount of bioturbation events, i.e., large N. The form (A32) can be re-arranged further to accommodate the drift of the random walker. To this end, we can rescale the coordinate axis introducing the new coordinate $z = x - v_b t$. Defining the concentration in this new coordinate as $\hat{C}(z, t) = C(x, t)$, the temporal derivative in the old and new coordinate system are related via

$$\frac{\partial C}{\partial t} = \frac{\partial \hat{C}}{\partial t} + \frac{\partial \hat{C}}{\partial z}\frac{\partial z}{\partial x} = \frac{\partial \hat{C}}{\partial t} - v_b \frac{\partial \hat{C}}{\partial z}. \tag{A36}$$

Upon substitution of (A36), the advective term vanishes in (A32), which then reduces to classical diffusion equation

$$\frac{\partial \hat{C}}{\partial t} = D_b \frac{\partial^2 \hat{C}}{\partial z^2} + \varepsilon(z, t). \tag{A37}$$

Because $\partial^n \hat{C}/\partial z^n = \partial^n C/\partial x^n$ the remainder term remains unchanged in the new and old coordinate system

$$\varepsilon(z, t) = \frac{1}{\tau_c} \sum_{n=3}^{\infty} \frac{(-1)^n}{n!} K_n \frac{\partial^n \hat{C}}{\partial z^n}. \tag{A38}$$

For this, it is useful to bring Eq. (A37) in a dimensionless form. To this end, we introduce the time scale T and length scale L over which the random walk is observed. By means of the dimensionless variables $\tilde{z} = z/L$, $\tilde{t} = t/T$, and $\tilde{C} = CL^3$, (A37) can be brought in the dimensionless form

$$\frac{\partial \tilde{C}}{\partial \tilde{t}} = \frac{\tau_{obs}}{\{\lambda_{obs}\}^2}\frac{\sigma^2}{2\bar{\tau}}\frac{\partial^2 \tilde{C}}{\partial \tilde{z}^2} + \frac{1}{\tau_c}\sum_{n=3}^{\infty}\frac{(-1)^n}{n!}\frac{\tau_{obs}}{\{\lambda_{obs}\}^n} K_n \frac{\partial^n \tilde{C}}{\partial \tilde{z}^n}. \tag{A39}$$

The crucial task is now to find appropriate expressions for the observational time scale τ_{obs} and the length scale λ_{obs}. These should be properly linked to the characteristic process scale λ_c and τ_c of the random walk. The appropriate relations are:

$$\tau_{obs} = \tau_c N \tag{A40}$$

$$\lambda_{obs} = \sigma \sqrt{N}. \tag{A41}$$

The link (A40) between the observational time scale and the process scale is straight forward: within the time frame of observation on average N events will occur. The determination of the observational length scale λ_{obs} however needs more explanation. When the number of events increases, the tracer profile will show increasingly more spreading. Accordingly, the length scale at which we observe the mixing will be dependent (1) on the number of mixing events N, and on the intrinsic displacement distance within a single event $\lambda_c = \sigma$. Upon substitution of both the relations (A40) and (A41) into (A39) we arrive at

$$\frac{\partial \tilde{C}}{\partial \tilde{t}} = \frac{1}{2}\frac{\partial^2 \tilde{C}}{\partial \tilde{z}^2} + \sum_{n=3}^{\infty} \frac{1}{n!}\frac{1}{N^{(n-2)/2}}\frac{K_n}{\sigma^n}\frac{\partial^n \tilde{C}}{\partial \tilde{z}^n}. \tag{A42}$$

Taking the limit for an infinite number of bioturbation events, we obtain

$$\lim_{N\mapsto+\infty}[\varepsilon(z, t)] = \lim_{N\mapsto+\infty}\left[\sum_{n=3}^{\infty}\frac{1}{n!}\frac{1}{N^{(n-2)/2}}\frac{K_n}{\sigma^n}\frac{\partial^n \tilde{C}}{\partial \tilde{z}^n}\right] = 0. \tag{A43}$$

Again, the "pseudo-diffusive" form points to a close connection between the general particle displacement model and the diffusion equation. This connection will be further explored in the next section.

APPENDIX G

Long-time behavior of the Montroll-Weiss walk

a. Laplace-Fourier transform of CTRW equation

To arrive at the diffusion equation, we start from the basic CTRW expression, (37) repeated,

$$C(x, t) = C_0(x)\left[1 - \int_0^t \Psi_T(\tau)d\tau\right] + \int_0^t \int_{-\infty}^{\infty} \Psi_T(\tau)\Psi_L(\lambda)C(x - \lambda, t - \tau)d\lambda d\tau \tag{A44}$$

which we will transform into Fourier-Laplace space. To this end, we can first apply the Fourier transform to (A44) with respect to spatial coordinate. Using the convolution theorem, we thus obtain

$$\hat{C}(k,\,t) = \hat{C}_0(k)\left[1 - \int_0^t \Psi_T(\tau)d\tau\right] + \int_0^t \Psi_T(\tau)\hat{\Psi}_L(k)\hat{C}(k,\,t-\tau)d\tau \tag{A45}$$

where the hat notation for the concentration is used to denote their Fourier transform

$$\hat{f}(k) \equiv \int_{-\infty}^{\infty} f(x)\exp(-ikx)dx \tag{A46}$$

with the inversion

$$f(x) = \frac{1}{2\pi}\int_{-\infty}^{\infty} \hat{f}(k)\exp(ikx)dk. \tag{A47}$$

In a second step, we apply the Laplace transform to (A45) with respect to time. Again using the convolution theorem, we arrive at

$$\hat{\tilde{C}}(k,\,s) = \frac{1}{s}\,(1 - \hat{\Psi}_T(s))\hat{C}_0(k) + \hat{\Psi}_T(s)\hat{\Psi}_L(k)\hat{\tilde{C}}(k,\,s) \tag{A48}$$

where the tilde notation denotes the Laplace transform

$$\tilde{f}(s) \equiv \int_0^{\infty} f(t)\exp(-st)dt \tag{A49}$$

with the inversion

$$f(t) = \frac{1}{2\pi i}\int_{\gamma-\infty}^{\gamma+\infty} \tilde{f}(s)\exp(st)ds \tag{A50}$$

where γ is a real number so that the contour path of integration is in the region of convergence of $\tilde{f}(s)$. By solving the algebraic (A48), we directly obtain the transform of the unknown concentration profile as

$$\hat{\tilde{C}}(k,\,s) = \frac{1 - \hat{\Psi}_T(s)}{s(1 - \hat{\Psi}_T(s)\hat{\Psi}_L(k))}\,\hat{C}_0(k). \tag{A51}$$

Eq. (A51) can be rewritten as

$$\hat{\tilde{C}}(k,\,s) = \frac{1 - \hat{\Psi}_T(s)}{s}\,\frac{\hat{C}_0(k)}{1 - \hat{\Psi}_T(s)\hat{\Psi}_L(k)} \tag{A52}$$

which is often referred to as the Montroll-Weiss equation.

b. Special case: Gaussian jump lengths and exponential waiting times

We can now investigate for the specific case where jump-length distribution is Gaussian, and the waiting-time distribution is exponential. The Laplace transform of the exponential waiting distribution, and the Fourier transform of the jump-length distribution respectively become

$$\hat{\Psi}_T(s) = \frac{1}{\bar{\tau}s + 1} \tag{A53}$$

$$\hat{\Psi}_L(k) = 1 - \frac{\sigma^2}{2} k^2. \tag{A54}$$

Upon substitution of (A53) and (A54) into (A52), and after some elementary re-arrangement, one obtains

$$\hat{\tilde{C}}(k, s) = \frac{1}{s + \frac{\sigma^2}{2\bar{\tau}} k^2} \hat{C}_0(k). \tag{A55}$$

When back-transformed to (x, t)-coordinates, the solution of (A55) approaches the solution of the classical diffusion equation for long times $t \to \infty$ (Hughes, 1995)

$$\frac{\partial C}{\partial t} = \frac{\sigma^2}{2\bar{\tau}} \frac{\partial^2 C}{\partial x^2} \tag{A56}$$

subject to the initial condition $C(x, 0) = C_0(x)$. In other words, after a small initial transition period, a bioturbation regime characterized the Gaussian jump length PDF and the exponential waiting time PDF becomes diffusive.

c. Long-time behavior of Montroll-Weiss random walk

We can now investigate the behavior a bioturbation regime characterized by a general jump length and waiting-time distributions. The Laplace transform of the general waiting-time distribution Ψ_T can be expanded as

$$\hat{\Psi}_T(s) \sim 1 + \left[\frac{d\hat{\Psi}_T}{ds}\bigg|_{s=0} \right] s + O(s^2). \tag{A57}$$

If the waiting time is finite, we can use the relation (Hughes, 1995)

$$\frac{d\hat{\Psi}_T}{ds}\bigg|_{s=0} = -\bar{\tau} = -\int_0^\infty \tau \Psi_T(\tau) d\tau. \tag{A58}$$

So the expansion immediately simplifies to

$$\hat{\Psi}_T(s) \sim 1 - \bar{\tau}s + O(s^2). \tag{A59}$$

Similarly, the Fourier transform of the symmetric jump-length distribution Ψ_L can be expanded as (Hughes, 1995)

$$\hat{\Psi}_L(k) \sim 1 - \frac{\sigma^2}{2} k^2 + O(k^4) \tag{A60}$$

where the variance σ^2 is defined through

$$\left.\frac{d\hat{\Psi}_L}{d^2k}\right|_{k=0} = -\sigma^2 = -\int_{\infty}^{\infty} \lambda^2 \Psi_L(\lambda) d\lambda. \tag{A61}$$

The asymptotic behavior of $C(x, t)$ for $t \to \infty$ is governed by the behavior of $\hat{\tilde{C}}(k, s)$ when $s \to 0$ and $k \to 0$ (Hughes, 1995 p. 285; Metzler and Klafter, 2000). Accordingly, upon substitution of (A59) and (A60) into (A52) and dropping the higher-order terms, we finally arrive at

$$\hat{\tilde{C}}(k, s) \approx \frac{1}{s + \dfrac{\sigma^2}{2\bar{\tau}} k^2} \hat{C}_0(k), \tag{A62}$$

which has exactly the same form as (A55) for the Gaussian jump length and exponential waiting-time distribution. Therefore, for long times $t \to \infty$, any bioturbation regime will become diffusive, as long as $\bar{\tau}$ and σ^2 remain finite quantities.

REFERENCES

Aller, R. C. 1982. The effects of macrobenthos on chemical properties of marine sediment and overlying water, *in* Animal-Sediment Relations, P. L. McCall and M. J. S. Tevesz, eds., Plenum, 53–102.

—— 1988. Benthic fauna and biogeochemical processes in marine sediments: The role of burrow structures, *in* Nitrogen Cycling in Coastal Marine Sediments, T. H. Blackburn and J. Sorensen, eds., John Wiley & Sons, 301–338.

Berg, H. C. 1993. Random Walks in Biology, Princeton University Press, 152 pp.

Berg, P., S. Rysgaard, P. Funch and M. K. Sejr. 2001. Effects of bioturbation on solutes and solids in marine sediments. Aquat. Microb. Ecol., *26,* 81–94.

Berner, R. A. 1980. Early Diagenesis: A Theoretical Approach. Princeton University Press, 241 pp.

Boudreau, B. P. 1989. The diffusion and telegraph equations in diagenetic modeling. Geochim. Cosmochim. Acta, *53,* 1857–1866.

—— 1986. Mathematics of tracer mixing in Sediments: I. Spatially-dependent, diffusive mixing. Am. J. Sci., *286,* 161–198.

—— 2005. Modelling mixing and diagenesis, *in* Interactions between Macro- and Microorganisms in Marine Sediments, E. Kristensen, J. E. Kostka and R. R. Haese, eds., American Geophysical Union, 323–340.

—— 1997. Diagenetic Models and Their Implementation. Springer, Berlin, 414 pp.

Boudreau, B. P. and D. M. Imboden. 1987. Mathematics of tracer mixing in sediments: III. The theory of nonlocal mixing within sediments. Am. J. Sci., *287,* 693–719.

Cadée, G. C. 2001. Sediment dynamics by bioturbating organisms, *in* Ecological Comparisons of Sedimentary Shores, K. Reise, ed., Springer, 127–148.

Cochran, J. K. 1985. Particle mixing rates in sediments of the eastern Equatorial Pacific—Evidence from Pb-210, Pu-239, Pu-240 and Cs-137 distributions at Manop sites. Geochim. Cosmochim. Acta, *49,* 1195–1210.

Crank, J. 1975. The Mathematics of Diffusion, Oxford University Press, 415 pp.

Crusius, J. and T. C. Kenna. 2007. Ensuring confidence in radionuclide-based sediment chronologies and bioturbation rates. Estuar. Coast. Shelf Sci., *71,* 537–544.

Delmotte, S., F. J. R. Meysman, A. Ciutat, A. Boudou, S. Sauvage and M. Gerino. 2007. Cadmium transport in sediments by tubificid bioturbation: An assessment of model Complexity. Geochim. Cosmochim. Acta, *71,* 844–862.

Feller, W. 1968. An Introduction to Probability Theory and its Applications, John Wiley & Sons, 509 pp.

Fernandes, S., F. J. R. Meysman and P. Sobral. 2006. The influence of Cu contamination on *Nereis Diversicolor* bioturbation. Mar. Chem., *102,* 148–158.

Fisher, J. B., W. J. Lick, P. L. McCall and J. A. Robbins. 1980. Vertical mixing of lake sediments by tubificid oligochaetes. J. Geophys. Res., *85,* 3997–4006.

Foster, D. W. 1985. BIOTURB: a Fortran program to simulate the effects of bioturbation on the vertical distribution of sediments. Comput. Geosci., *11,* 39–45.

Francois, F., J. C. Poggiale, J. P. Durbec and G. Stora. 1997. A new approach for the modelling of sediment reworking induced by a macrobenthic community. Acta Biotheor., *45,* 295–319.

—— 2001. A new model of bioturbation for a functional approach to sediment reworking resulting from macrobenthic communities, *in* Organism-Sediment Interactions, J. Y. Aller, S. A. Woodin and R. C. Aller., eds., University of South Carolina Press, 75–88.

Goldberg, E. D. and M. Koide. 1962. Geochronological studies of deep-sea sediments by the Io/Th method. Geochim. Cosmochim. Acta, *26,* 417–450.

Guinasso, N. L. and D. R. Schink. 1975. Quantitative estimates of biological mixing rates in abyssal sediments. J. Geophys. Res.-Ocean. Atmos., *80,* 3032–3043.

Herman, P. M. J., J. J. Middelburg, J. Van De Koppel and C. H. R. Heip. 1999. Ecology of estuarine macrobenthos. Adv. Ecol. Res., *29,* 195–240.

Hughes, B. D. 1995. Random walks and Random Environments. Volume 1: Random Walks. Clarendon Press, 631 pp.

Jumars P. A., A. R. M. Nowell and R. F. L. Self. 1981. A simple-model of flow-sediment-organism interaction. Mar. Geol., *42,* 155–172.

Kot, M., M. A. Lewis and P. van den Driessche. 1996. Dispersal data and the spread of invading organisms. Ecology, *77,* 2027–2042.

Lecroart, P., O. Maire, S. Schmidt, A. Grémare, P. Anschutz and F. J. R Meysman. 2010. Bioturbation, short-lived radioisotopes, and the tracer-dependence of biodiffusion coefficients. Geochim. Cosmochim. Acta, *74,* 6049–6063.

Lecroart, P., S. Schmidt, P. Anschutz and J. M. Jouanneau. 2007. Modeling sensitivity of biodiffusion coefficient to seasonal bioturbation. J. Mar. Res., *65,* 417–440.

Levin, S. A, H. C. Muller-Landau, R. Nathan, J. Chave. 2003. The ecology and evolution of seed dispersal: a theoretical perspective. Ann. Rev. Ecol. Evol. Syst., *34,* 575–604.

Maire O., J. C. Duchene, A. Gremare, V. S. Malyuga and F. J. R. Meysman. 2007. A comparison of sediment reworking rates by the surface deposit-feeding bivalve *Abra Ovata* during summertime and wintertime, with a comparison between two models of sediment reworking. J. Exp. Mar. Biol. Ecol., *343,* 21–36.

Matisoff, G. 1982. Mathematical models of bioturbation, *in* Animal-Sediment Relations, R. L. McCall and M. J. S. Tevesz, eds., Plenum Press, 289–330.

Meile C. and P. Van Cappellen. 2005. Particle age distributions and O_2 exposure times: Timescales in bioturbated sediments. Glob. Biogeochem. Cycles, *19,* Art. No. GB3013.

Metzler, R. and J. Klafter. 2000. The Random Walk's guide to anomalous diffusion: A fractional dynamics approach. Phys. Rep.-Rev. Sec. Phys. Lett., *339,* 1–77.

Meysman, F. J. R., B. P. Boudreau and J. J. Middelburg. 2003. Relations between local, nonlocal, discrete and continuous models of bioturbation. J. Mar. Res., *61,* 391–410.

—— 2005. Modeling reactive transport in sediments subject to bioturbation and compaction. Geochim. Cosmochim. Acta, *69,* 3601–3617.

Meysman, F. J. R., V. S. Malyuga, B. P. Boudreau and J. J. Middelburg. 2008a. A generalized stochastic approach to particle dispersal in soils and sediments. Geochim. Cosmochim. Acta, *72,* 3460–3478.

—— 2008b. Quantifying particle dispersal in aquatic sediments at short time scales: model selection. Aquatic Biology, *2,* 239–254.

Meysman, F. J. R., J. J. Middelburg and C. H. R. Heip. 2006. Bioturbation: A fresh look at Darwin's last idea. Trends Ecol. Evol., *21*, 688–695.

Montroll, E. W. and G. H. Weiss. 1965. Random walks on lattices, II. J. Math. Phys., *6,* 167–181.

Mulsow, S., B. P. Boudreau and J. N. Smith. 1998. Bioturbation and porosity gradients. Limnol. Oceanogr., *43,* 1–9.

Murray, J. D. 1989. Mathematical Biology, Springer, 537 pp.

Okubo, A. and S. A. Levin. 2001. Diffusion and Ecological Problems: New Perspectives, 2nd ed., Springer, 467 pp.

Othmer, H. G., S. R. Dunbar and W. Alt. 1988. Models of dispersal in biological systems. J. Math. Biol., *26,* 263–298.

Pearson, K. 1905. The problem of the Random Walk. Nature, *72,* 294.

Reed, D. C., K. Huang, B. P. Boudreau and F. J. R. Meysman. 2006. Steady-state tracer dynamics in a lattice-automaton model of bioturbation. Geochim. Cosmochim. Acta, *70,* 5855–5867.

Reed, D. C., B. P. Boudreau and K. Huang. 2007. Transient tracer dynamics in a lattice-automaton model of bioturbation. J. Mar. Res., *65,* 813–833.

Rice, D. L. 1986. Early diagenesis in bioadvective sediments—Relationships between the diagenesis of Beryllium-7, sediment reworking rates, and the abundance of conveyor-belt deposit-feeders. J. Mar. Res., *44,* 149–184.

Richter, R. 1952. Fluidal-texture in sediment-Gesteinen und ober Sedifluktion uberhaupt. Notizbl. Hess. L.-Amt. Bodenforsch., *3,* 67–81.

Risken, H. 1996. The Fokker-Planck Equation: Methods of Solution and Application. Springer, 427 pp.

Robbins, J. A. 1986. A model for particle-selective transport of tracers in sediments with conveyor belt deposit feeders. J. Geophys. Res., *91,* 8542–8558.

Shull, D. H. 2001. Transition-matrix model of bioturbation and radionuclide diagenesis. Limnol. Oceanogr., 46, 905–916.

Soetaert K., P. M. J. Herman, J. J. Middelburg, C. Heip, H. S. Destigter, T. C. E. Vanweering, E. Epping and W. Helder. 1996. Modeling Pb-210-Derived Mixing Activity in Ocean Margin Sediments: Diffusive Versus Nonlocal Mixing. J. Mar. Res., *54,* 1207–1227.

Solan, M. and B. D. Wigham. 2005. Biogenic particle reworking and bacterial-invertebrate interactions in marine sediments, *in* Interactions between Macro- and Microorganisms in Marine Sediments, E. Kristensen, J. E. Kostka and R. R. Haese., eds., Am. Geophys. Union, 105–124.

Solan, M., B. D. Wigham, I. R. Hudson, R. Kennedy, C. H. Coulon, K. Norling, H. C. Nilsson and R. Rosenberg. 2004. *In Situ* quantification of bioturbation using time-lapse fluorescent sediment

profile imaging (F-Spi.), luminophore tracers and model simulation. Mar. Ecol. Prog. Ser., *271,* 1–12.

Swift D. J. P., J. K. Stull, A. W. Niedoroda, C. W. Reed and G. T. F. Wong. 1996. Contaminant dispersal on the Palos Verdes continental margin. 2. Estimates of the biodiffusion coefficient, D-B, from composition of the benthic infaunal Community. Sci. Total Environ., *179,* 91–107.

Trauth, M. H. 1998. Turbo: A dynamic-probabilistic simulation to study the effects of bioturbation on paleoceanographic time series. Comput. Geosci., *24,* 433–441.

Van Cappellen, P. and Y. F. Wang. 1996. Cycling of iron and manganese in surface sediments: A general theory for the coupled transport and reaction of carbon, oxygen, nitrogen, sulfur, iron, and manganese. Am. J. Sci., *296,* 197–243.

Wheatcroft R. A., P. A. Jumars, C. R. Smith and A. R. M. Nowell. 1990. A mechanistic view of the particulate biodiffusion coefficient—Step lengths, rest periods and transport directions. J. Mar. Res., *48,* 177–207.

Received: *22 October, 2009;* revised: *8 March, 2011.*